Advanced Materials '93, VI / Frontiers in
Materials Science and Engineering, edited by S. Sōmiya et al.
Trans. Mat. Res. Soc. Jpn., Volume 19B
1994 Elsevier Science B.V.

HIGH STRENGTH MICROALLOYED ALUMINIUM ALLOYS

B.C. Muddle, S.P. Ringer* and I.J. Polmear

Department of Materials Engineering, Monash University, Clayton, Victoria, 3168, Australia

The emergence of a new class of high strength (0.2% proof stress 450-500 MPa) and ultra-high strength (0.2% proof stress up to 700MPa) aluminium alloys for use in structural applications in the aircraft and aerospace industries is reviewed. In this important class of alloys, the tensile yield strength is attributable to precipitation strengthening associated predominantly with the formation of nano-scale (<2 nm thickness), metastable plate-shaped precipitates on either {100} or {111} planes of an aluminium matrix. The identity and distribution of these precipitates may be controlled by microalloying additions and, in some cases, plastic deformation prior to the precipitation hardening treatment. The design of these alloys is examined and those factors important to controlling their precipitation behaviour and thus potential for strengthening are discussed. Particular emphasis is given to alloys based on the Al-Cu(-Li) system, microalloyed with additions of Mg and Ag, but attention is also drawn to the marked similarities that characterise the structures and mode of formation of the intermediate phases that control the strength of alloys in this class.

1. INTRODUCTION

Ultra-high strength aluminium alloys are used extensively in the aircraft and aerospace industries in applications requiring high specific strength, stiffness, fracture toughness and fatigue resistance. With continuing emphasis on weight reduction and increased operating speeds and altitudes for advanced aircraft, and mounting competitive pressures from non-metallic composite materials, there is an ongoing imperative for the design and development of new and improved alloys, which combine improved mechanical properties at both ambient and elevated temperatures (100-200°C) with economic advantages over competing materials.

Conventional high strength, structural aluminium alloys achieve their strength via the process of precipitation hardening [e.g. 1], which requires an alloy in which the solute element(s) exhibit decreasing solubility with decreasing temperature, Figure 1 [2]. Maximum strength and hardness are achieved as a result of a two-stage heat treatment involving a high temperature solution treatment in the temperature range ΔT_1 (500-550°C) and water quench, followed by one or two ageing treatments of the retained supersaturated solid solution in the lower temperature range ΔT_2 (130-200°C). The microstructures developed during the ageing treatment comprise a nano-scale (typically <10 nm) dispersion of precipitate particles reinforcing an aluminium matrix. The decomposition of the supersaturated solid solution during ageing is commonly a complex process involving several stages and control of the ageing conditions is important to optimise the resulting precipitate dispersion and thus mechanical properties. The duration of the ageing treatment is particularly critical, for beyond the ageing time required for maximum strength the alloys are said to 'overage' and the strength and hardness decrease significantly. The strengthening precipitate particles coarsen and become less effective in reducing dislocation mobility. For this reason, conventional high strength alloys cannot be used at temperatures above 100-150°C, for their mechanical properties deteriorate rapidly with elevated temperature

* Present Address: Institute for Materials Research, Tohoku University, 2-1-1 Katahira Aoba-ku, Sendai 980, JAPAN.

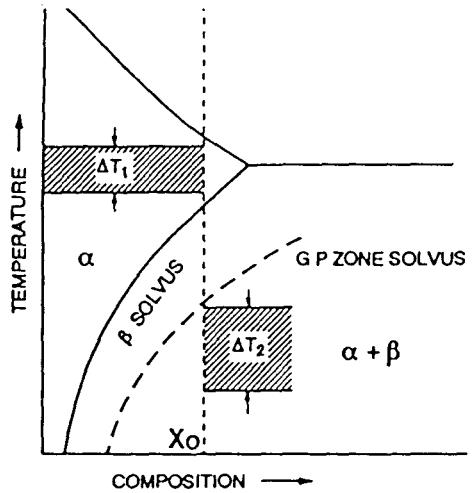

Figure 1. Schematic phase diagram typical of potential precipitation hardening binary system, showing temperature ranges for solution treatment (ΔT_1) and ageing (ΔT_2) for an alloy of composition X_o [2].

exposure.

The purpose of the present paper is to provide a brief review of ideas behind the emergence of an important new class of alloys, in which the high tensile yield strength (500-750 MPa) is attributable to precipitation strengthening associated predominantly with intermediate metastable phases forming as very fine-scale, thermally stable plate-.shaped precipitates on either $\{100\}_\alpha$ or $\{111\}_\alpha$ planes of the α-Al matrix phase

A feature of these alloys, based principally on the Al-Cu(-Li) and Al-Zn-Mg(-Cu) systems, is the degree to which the precipitation behaviour and thus properties may be influenced and controlled by microalloying additions of elements such as Cd, In, Sn, Mg, Zr and Ag [3,4]. A common practice in the physical metallurgy of low alloy steels for some considerable time [5], the application of microalloying additions in the design of advanced commercial aluminium alloys has not been as widely exploited [6] and has considerable potential for future development.

In the design of precipitation-strengthened alloys, the maximum potential for strengthening is commonly considered to occur when an alloy contains precipitates that have a structure and size sufficient to resist shearing and yet are too finely-spaced to be by-passed by dislocations [7,8]. This critical situation has proven difficult to achieve in practical alloys and the maximum strengthening response is usually observed when the microstructure contains a combination of coherent, shearable solute clusters or zones and relatively widely spaced metastable, intermediate precipitates. Examples include binary Al-Cu and ternary Al-Cu-Mg alloys, where peak hardness is associated with the presence of finely-dispersed, coherent zones (θ" or GP (Cu,Mg) respectively) and partly-coherent precipitates (θ' or S respectively), each of the latter nucleating preferentially on dislocations. The GP zones comprise clusters of solute atoms on $\{100\}_\alpha$ planes of the α-Al matrix phase, while the metastable, tetragonal θ" and θ' phases form as thin, partially-coherent plates on $\{100\}_\alpha$ and the S phase takes the form of sheets or assemblies of fine rods on $\{210\}_\alpha$ planes, elongated in $<100>_\alpha$ directions.

One way to achieve a more refined, uniform dispersion of intermediate precipitates, which resist shearing by dislocations during deformation, is to strain alloys prior to ageing (T8 temper) and increase the density of dislocations on which the precipitates form. A second approach, of more limited application, involves duplex ageing initially below and then above the GP zone solvus temperature to promote nucleation of higher temperature, intermediate precipitates at the sites of stable GP zones (e.g. T73 temper in Al-Zn-Mg-Cu alloys [1]). In some aluminium alloys, specific trace elements can also stimulate nucleation of refined dispersions of intermediate precipitates. One well known example is the effect of minor additions of Cd, In or Sn, all of which increase the strength and hardness of artificially aged Al-Cu alloys by promoting nucleation of a finer, more uniform dispersion of the phase θ' [9,10]. A more general effect is that involving trace additions of Ag, which can promote a greater response to age hardening in all aluminium alloys containing Mg [11-15]. The mechanisms involved appear to differ with different alloy systems. Silver may stimulate an existing ageing process (e.g. η' formation in Al-Zn-Mg and Al-Zn-Mg-Cu alloys [11]), induce precipitation in compositions in which it is normally absent (e.g. Al-Mg alloys containing <5% Mg [12]), or change the actual precipitates that

form (e.g. Al-Cu-Mg alloys [13-15]).

In Al-Cu-Mg alloys with high Cu:Mg ratios (e.g Al-4%Cu-0.3%Mg), minor additions of Ag (0.1-0.5%) promote the formation of a novel precipitate phase, now commonly designated Ω [16-19]. The Ω phase forms as thin plates on the $\{111\}_\alpha$ planes and co-exists with minor fractions of precipitates such as θ" and θ' (Al_2Cu), which form on the $\{100\}_\alpha$ planes in binary Al-Cu alloys. It has been shown to be the predominant strengthening phase in the commercial alloy 201 (Al-4.5%Cu-0.35%Mg-0.7%Ag), which is the strongest of all aluminium casting alloys [1]. It is also the primary constituent of a new wrought alloy (Al-6.5%Cu-0.45%Mg-0.4%Ag-0.3%Mn-0.15%Zr), which combines high room temperature strength (T6 0.2% proof stress 520 MPa), with improved creep properties in the range 150-220°C [20]. Designed initially for possible use in compressor wheels for superchargers and load-based gas turbines, this alloy has since been shown to be weldable and thus a potential replacement for the well-known lower strength alloy 2219 (T6 0.2% proof stress 300MPa) in certain aerospace applications, such as cryogenic fuel tanks or the fuselage of supersonic passenger aircraft.

In a further development in the quest for higher strength alloys, it has recently been reported [21-23] that small additions of Li (1.0-1.5%) to Al-Cu-Mg-Ag alloys may stimulate a still greater age hardening response and an alloy known as Weldalite 049™ (Al-6.3% Cu-1.3% Li- 0.4% Mg-0.4% Ag-0.18% Zr) has been shown to have a tensile yield strength that may exceed 700 MPa [22]. Special interest is now centred on the mechanism by which the Al-Cu-Li-Mg-Ag alloys develop such high strength. Transmission electron microscopy has revealed the presence of significant volume fractions of at least three precipitates, which resist shearing by dislocations, in the peak-aged microstructures of such alloys. These were initially identified as Ω, θ' and S' (Al_2CuMg) [21], but in recent work [23,24] it has become clear that the hexagonal phase T_1 (Al_2CuLi) or a 'T_1-like' phase replaces all or some of the Ω phase as the primary strengthening phase in the Li-containing alloys. The Ω and T_1 phases both form as thin, hexagonal plates on $\{111\}_\alpha$ and are sufficiently similar structurally to be difficult to distinguish using conventional imaging and diffraction techniques. It has been suggested [21] that it is the combination of the three phases T_1 (or Ω), θ' and S (or S') formed on different crystal planes that is perhaps unique to this alloy and responsible for the exceptional hardening that is observed.

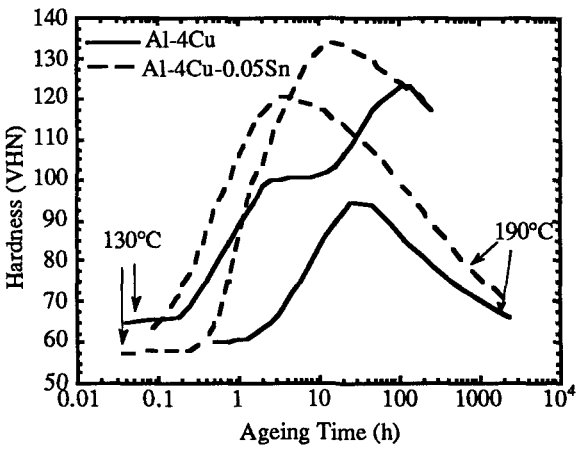

Figure 2. Variation in hardness (VHN) with ageing time for an Al - 4 wt% Cu alloy, with and without additions of 0.05 wt% Sn, at ageing temperatures of 130°C and 190°C. [9, 30-32].

2. ALLOYS OF THE Al-Cu SYSTEM

2.1. Binary Al-Cu Alloys

Precipitation hardening has been studied more extensively in Al-Cu alloys than any other light alloy system and although there are now few commercial alloys based on this system, it provides an important reference point, both historically and technically. Furthermore, despite intense research efforts, much remains unknown about the mechanisms surrounding the nucleation and growth of precipitates in Al-Cu, and certain structural details are also unresolved. The solid curves in Figure 2 show the precipitation hardening response typical of a binary Al - 4wt% Cu alloy, solution treated, quenched and aged isothermally at 130°C and 190°C. The age hardening response is attributable [25] to the formation of a series of metastable, intermediate precipitate phases during decomposition of supersaturated α solid solution, the precipitation sequence involving formation of Guinier-Preston (GP) I zones → GP II zones (or θ" phase) → metastable θ' → equilibrium θ phase. With the exception of the equilibrium phase, each of the

precipitate phases in binary Al-Cu alloys is a plate-shaped product formed parallel to $\{100\}_\alpha$ planes.

At 130°C, two stages of hardening are observed, reflecting a complex sequence of precipitation. The initial rise in hardness is attributed to the formation of GP I zones, which are commonly described [26-29] as single-atom layer clusters of copper atoms parallel to $\{100\}_\alpha$. These copper rich clusters are coherent with the matrix and give diffraction effects typical of a two dimensional lattice. They are thought to form spontaneously on quenching from the solution treatment temperature and may be thermally stable up to approximately 140-160°C. The hardening that occurs during natural (room temperature) ageing for periods up to three years (and probably indefinitely) is attributed entirely to their presence [28]. Once the GP I zones reach a critical diameter (between 5 and 10 nm), a period of incubation commences, during which the zone diameter and hardness remain constant [28,30,31], resulting in a prominent hardness plateau. The second rise in hardness is attributed to θ'' precipitation, usually as a result of the allotropic transformation of GP I zones, although it has been shown [28] that under suitable conditions of supersaturation, GP I zones, θ'', θ' and θ in turn can nucleate directly from the matrix.

The θ" phase again takes the form of plate-shaped precipitates parallel to $\{100\}_\alpha$ planes. It has a tetragonal (t) crystal structure defined by layers of copper atoms parallel to the basal plane, separated by three layers of aluminium atoms. It is initially fully coherent with the α matrix, both within the basal plane (parallel to the habit plane) and normal to it. However, during ageing the θ" platelets increase in size and there is a reduction in the c_t parameter and an increase in the misfit strain normal to the habit plane, accompanied by an increase in alloy hardness. Peak hardness in such alloys is commonly associated with formation of a mix of such fine-scale θ" platelets (10 nm thick by 100 nm dia.), together with coarser $\{100\}_\alpha$ plates of metastable θ'. A less prominent hardness plateau is observed at peak hardness and this is the result of the progressive replacement of θ" by θ'. The θ' phase is also tetragonal, with $a_t \sim 0.404$ nm $\sim a_\alpha$ and $c_t \sim 0.580$ nm, and is thus coherent with the matrix α in the basal plane, which is parallel to the $\{100\}_\alpha$ habit plane, but semi-coherent normal to the habit plane. Prolonged ageing leads to the growth of larger θ' plates, which eventually undergo a loss of coherency and this, together with the gradual precipitation of the equilibrium θ phase, leads to a softening of the alloy (overageing).

It is observed that the first hardness plateau of the ageing curve becomes less prominent as the degree of supersaturation is reduced. Figure 2 shows that the ageing response in Al-4Cu has become a single stage process at 190°C, and accompanying the approach to a single peak hardness curve with decreasing supersaturation is a lower peak hardness compared to that with two stage ageing. The peak hardness values of binary Al-Cu alloys aged at various temperatures have been shown [30,31] to fall into two regimes depending on whether two stage ageing or single stage ageing is observed. Higher peak hardness values are associated with the presence of θ", whilst lower values arise when the precipitate phase is almost entirely θ', leading to a suggestion [28] that θ" provides greater hardening than does θ'. However, in comparing the properties arising from θ' and θ" dispersions this may be misleading, since the higher hardness in the group of alloys displaying two stage hardening could simply be the result of a higher number density of θ" precipitates. This must be compared with the θ' dispersion that occurs in single stage hardening at lower supersaturations with some degree of caution, as the latter may be softer because of the properties of the dispersion and not as a result of any intrinsic property associated with the ability of a particular precipitate phase to inhibit deformation.

2.1.1. Microalloying: Effects of Sn, In and Cd

The effects of a microalloying addition of Sn on the precipitation hardening response of Al-Cu alloys is also shown in Figure 2. For an ageing temperature of 190°C, the presence of as little as 0.05 wt% Sn leads to an accelerated rate of ageing and a substantial increase in peak hardness, while at 130°C hardening becomes a single stage process, with a reduction in the time to peak hardness and a significant increase in the maximum hardness achieved. Similar effects are found to a lesser extent in alloys with lower supersaturations, while microalloying additions of Cd and In produce similar effects both quantitatively and qualitatively.

Trace additions of Sn, Cd or In to Al-Cu appear

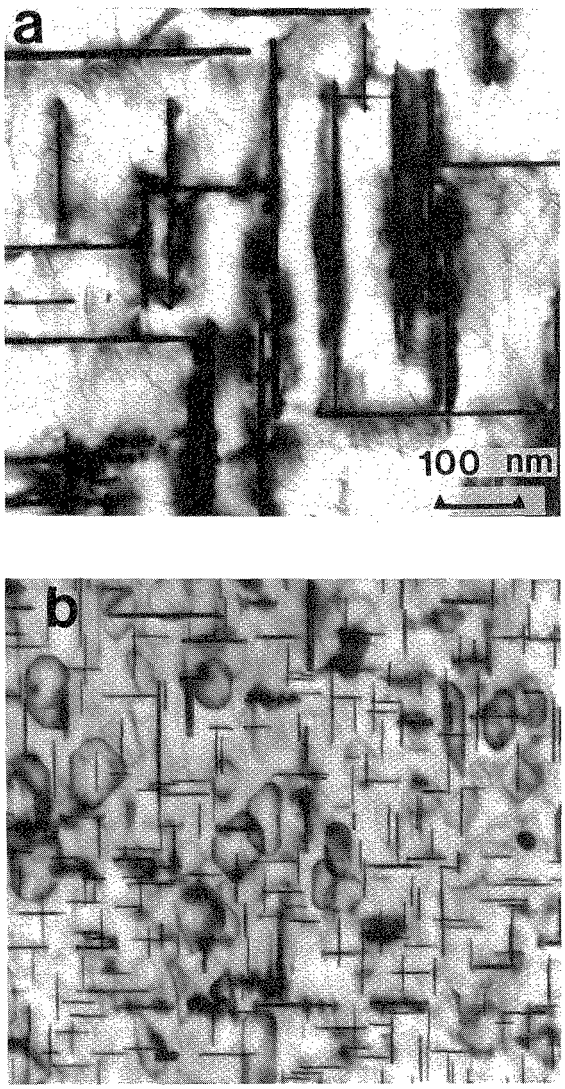

Figure 3. Transmission electron micrographs comparing the θ' precipitate distribution in an Al-4wt% Cu alloy, with and without an addition of 0.05 wt% Sn, after ageing for 18 h at 190°C (courtesy Gao Xiang).

to retard the formation of GP zones, as the ternary trace-modified alloys are observed to age harden more slowly than the binary alloys at ambient temperature [9]. At elevated ageing temperatures, the microalloying additions are thought to favour the formation of fine-scale θ' phase at the expense of GP zones and θ" [32]. The θ' observed in association with peak hardness in the ternary alloys is present in a refined and more uniform dispersion than the θ' observed in binary alloys. Figure 3 includes electron micrographs comparing the microstructures of an Al - 4wt% Cu alloy, with and without an addition of 0.05 wt% Sn, after ageing for 18 h at 190°C, and illustrates clearly the refined nature of the θ' present in the trace-modified alloy after an equivalent ageing treatment. The role of the microalloying additions in influencing the precipitation behaviour remains incompletely understood. It has been suggested that θ' nucleates preferentially at the sites of atom clusters stabilised by Sn, Cd, or In, or that these trace elements modify the θ' structure so as to reduce the precipitate/matrix interfacial energy and thus the energy barrier to nucleation [33-36]. However, there is currently little experimental evidence to distinguish between these possibilities.

Cold working of these alloys, post solution treatment and prior to ageing (T8 temper), has a strong effect on their age hardening response. The hardness and tensile strengths of binary Al-Cu alloys are increased, whereas these properties are reduced in the ternary trace-modified alloys. Detailed, but mostly qualitative, evaluations of the hardening process [32] suggest that the dislocations introduced during cold working provide preferred heterogeneous nucleation sites for θ' and thus promote the formation of θ'. In binary alloys, the T8 temper produces a fine dispersion of the θ' precipitate at the expense of θ", whereas the very fine dispersions of θ' present in undeformed trace-modified alloys is replaced by a comparatively coarser distribution. On this basis, a given dispersion of θ' precipitates may well cause greater hardening than the equivalent dispersion of θ". This may explain the higher hardness of undeformed ternary alloys (fine θ' at peak hardness) when compared with that of undeformed binary alloys (fine θ" at peak hardness) [28,32]. However, systematic studies which identify the main strengthening phases and which describe quantitatively the type of dispersion most effective in hardening are still lacking for those alloys strengthened primarily by plate-shaped precipitate phases.

2.1.2. Commercial Al-Cu Alloys

Table 1 provides a summary of the principal

Table 1
Tensile Property Comparisons of Selected High Strength Aluminium Alloys

Alloy	Heat Treatment	0.2% Proof Stress (MPa)	Tensile Strength (MPa)	% Elongation
2011: Al-5.5Cu(-0.7Fe-0.4Si-0.3Zn+Bi, Pb)	T6	295	390	17
2025: Al-4.5Cu(-1Fe-1Si-1Mn-0.25Zn+Cr, Mg, Ti)	T6	255	400	19
2219: Al-6.3Cu(-0.3Fe-0.2Si-0.3Mn+Mg, Zn, Ti, V, Zr)	T6	300	420	9
	T8	350	450	7
2017: Al-4Cu-0.6Mg(-0.7Fe-0.7Si-0.7Mn(-+Zn, Cr, Ti, Zr)	T4	275	425	22
2014: Al-4Cu-0.5Mg(-0.7Fe-0.9Si-0.8Mn+Zn, Cr, Ti)	T6	410	480	13
2021: Al-6.3Cu(-0.3Fe-0.2Si-0.3Mn-0.1Cd+Mg, Ti, Zr)	T6	435	505	9
2024: Al-4Cu-1.5Mg(-0.5Fe-0.5Si-0.5Mn-+Zn, Cr, Ti)	T4	325	470	20
	T6	395	475	10
	T8	450	480	6
Al-6.3%Cu-0.45%Mg-0.4%Ag (Extruded Rod)	T6	520	585	7.5
Weldalite ™ 049: Al-6.3Cu-1.3Li-0.4Mg-0.4Ag(+Zr)				
20°C Extruded Rod	T6	683	718	4
Extruded Rod	T8	696	715	5.5
Extruded Plate	T6	725	740	9
Sheet	T8	650	665	5
-196°C Extruded Plate	T8	783	840	8
7075: Al-5.6Zn-2.5Mg-1.5Cu(-0.5Fe-0.4Si-0.3Mn+Cr, Ti, Zr)	T6	500	570	11
	T73	430	500	13
	T76	470	540	12
7079: Al-4.4Zn-3.3Mg-0.6Cu(-0.4Fe-0.3Si-0.2Mn+Cr, Ti)	T6	470	540	12
7091: (Powder Metall.) Al-6.4Zn-2.5Mg-1.4Cu(+Fe, Si, Co, O)	T7E69	545	590	11

mechanical properties of the more prevalent commercial Al-Cu based alloys. Alloy 2011 is widely used where machining is necessary as it contains Bi and Pb additions, which aid machineability. Alloy 2025 has been used for forging applications, although it has largely been replaced by alloy 2219. The higher Cu content in alloy 2219, together with the lower Fe and Si levels, provide for higher ambient temperature tensile properties together with superior creep strength at elevated temperatures. Figure 4 shows the change in 0.2% proof stress with temperature for selected

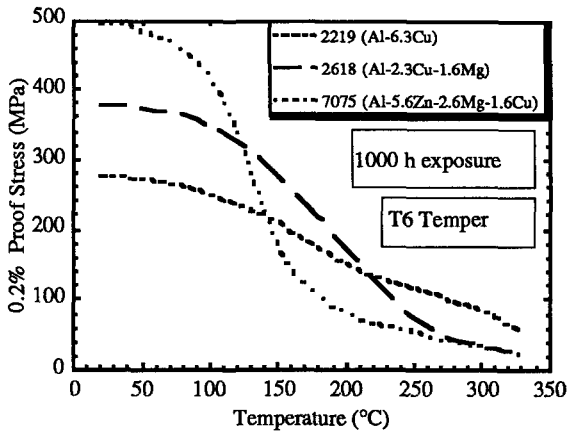

Figure 4. Variation in 0.2% proof stress with temperature after 1000 h exposure to elevated temperature for selected commercial aluminium alloys. [80].

alloys after 1000 h exposure to elevated temperature. Above approximately 220°C, alloy 2219 displays greater mechanical strength than comparable Al-Cu-Mg and Al-Zn-Mg alloys, although its room temperature tensile properties are much lower, Table 1. Alloy 2219 possesses a high toughness at cryogenic temperatures; it is available as sheet, plate or extrusions and is weldable. It has been used for

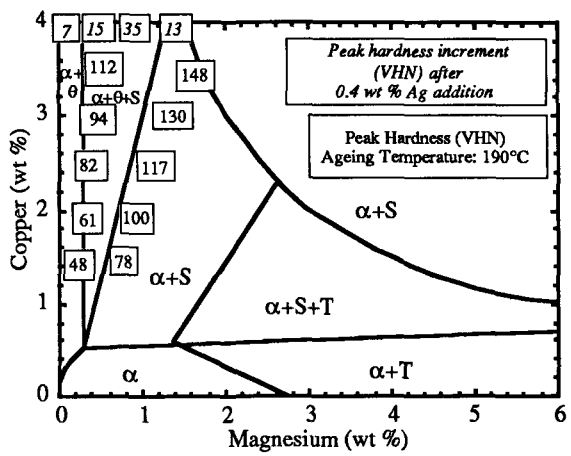

Figure 5. Aluminium-rich corner of the Al-Cu-Mg ternary phase diagram showing the phases present as a function of composition after long term ageing at 190°C. [37, 40].

fuel tanks for storing liquified gases that serve as rocket propellants and, as seen in Table 1, has a considerably enhanced response to age hardening in the T8 condition.

Alloy 2021 was developed with the aim of utilising the beneficial effects on the age-hardening response of microalloying additions of Sn, Cd or In. Based on the 2219 composition, it contains traces of Cd and Sn, and is suitable for more demanding applications where improved tensile properties are required. Another advantage of this material is that extrusion speeds may be 2-3 times faster than those for the equivalent Al-Cu-Mg alloys such as duralumin [1], because of the absence of Mg and the fact that it remains relatively soft and ductile in the solution treated and quenched condition when compared to conventional Al-Cu and Al-Cu-Mg alloys, where rapid GP zone formation occurs at room temperature. It may also be heat treated so as to be immune to stress corrosion cracking. Both 2219 and 2021 are good examples of high strength alloys that rely on the manipulation of complex age hardening processes. However, some countries have banned production of 2021 because Cd is regarded as a toxic hazard.

2.2. Al-Cu-Mg Alloys

The first commercial age-hardening aluminium alloy, the well known duralumin (Al-3.5Cu-0.35Mg), was developed in 1906 and, in spite of extensive research into airframe materials since this discovery, modern aircraft stuctures still contain components made from a very similar alloy (2017, Table 1). Although they do not possess an age hardening response equivalent to competing, high strength Al-Zn-Mg alloys for aircraft applications, Al-Cu-Mg alloys maintain advantages over Al-Zn-Mg alloys for applications involving exposure to temperatures greater than 100°C, Figure 4. This has become particularly significant with the development of supersonic aircraft, where increased velocities and altitudes lead to aerodynamic heating of certain parts of the skin and airframe to temperatures as high as 100-130°C.

Figure 5 shows the phases present in the Al-Cu-Mg system after long term ageing at 190 °C [37]. A feature of the diagram, is the wide range of temperature and composition over which the S (or

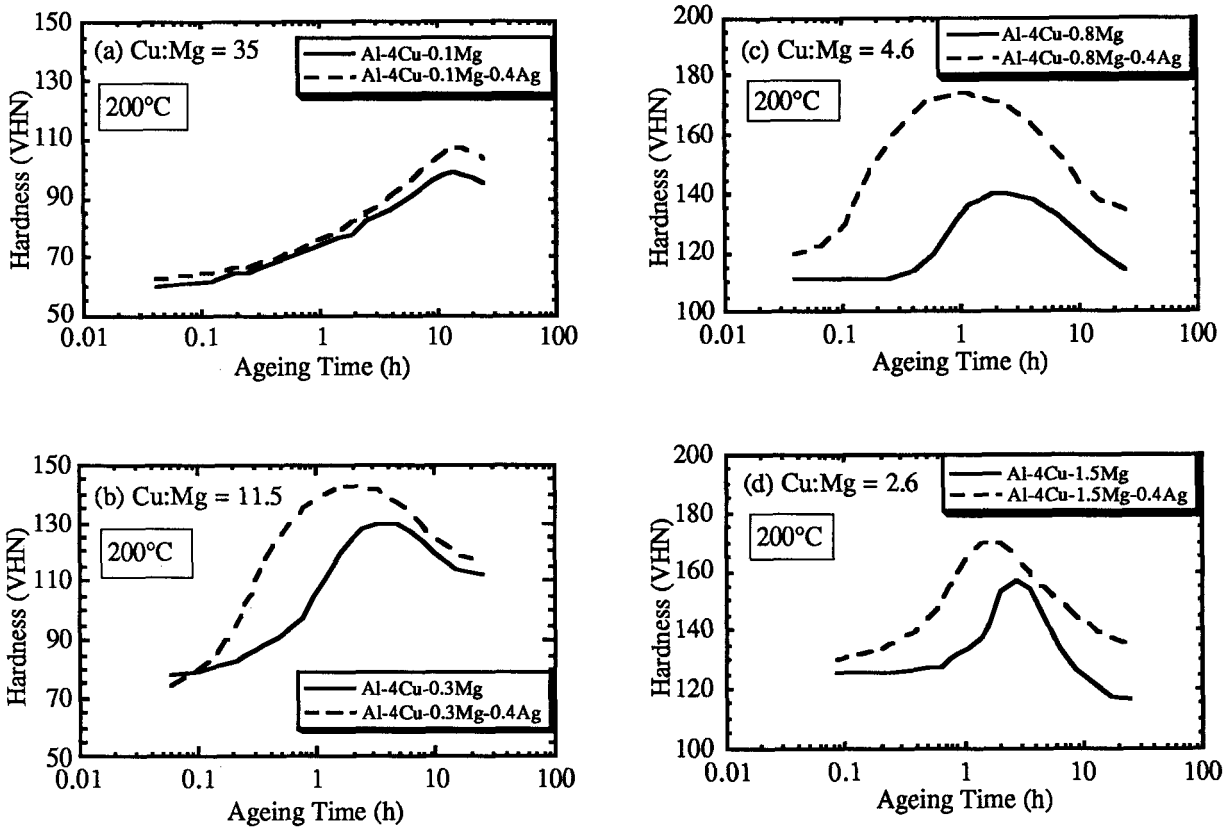

Figure 6 (a-d). Variation in hardness with ageing time at 200°C for a series of Al-Cu-Mg alloys with varying Cu:Mg ratios. In each case, solid curves represent Ag-free alloy, while dashed curves represent alloy containing 0.4 wt% Ag. [40].

S') phase (Al_2MgCu) is observed. The other equilibrium precipitate phases of significance are the θ phase (Al_2Cu), and a ternary T phase (Al_6CuMg_4). Most alloy development has focused on alloys with Cu:Mg weight ratios ≥ 1.5:1, which fall within the (α+S) and (α+θ+S) phase fields. Typical maximum hardness values (VHN) for ternary alloys in this range are superimposed on the phase diagram in Figure 5, and show that there is a significant increase in the hardness achieveable with an increase in Mg content and with increasing Cu:Mg ratio. In alloys having Cu:Mg ratios in excess of approximately 6.5:1 (α+θ+S alloys), the precipitation processes that occur are similar to those in binary Al-Cu alloys, together with those specific to the ternary system. In addition, the Ω phase, which forms as thin, hexagonal-shaped plates on the $\{111\}_\alpha$ planes has been observed, although only in small volume fractions in alloys that are aged at relatively high temperatures [38,39]. In those alloys having lower Cu:Mg ratios, the age-hardening response is attributable to ternary element precipitates almost exclusively.

Figure 6 [40] includes hardness curves which show the ageing response for a series of ternary alloys at 200°C, with the Cu:Mg ratio decreasing systematically from (a) to (d). In each alloy there is an initial rapid increase in hardness (typically 10-30 VHN above the as-quenched value), which is associated with the formation of ternary Guinier-

Preston zones, rich in Cu and Mg, and commonly referred to as GPB zones. A subsequent period of incubation is then followed by a rise to maximum hardness, which is attributed to the appearance of metastable S' and/or S phase precipitates. Hardness decreases rapidly during overageing as the GPB zones give way to S' or S phase.

There are two striking features of GPB zones, which are reflected in Figures 6 (a)-(d). The first is their very rapid rate of formation, compared to GP I zones, while the second concerns the wide range of thermal stability exhibited. GPB zones are easily detected at 200°C, and have been found in alloys aged at temperatures as high as 240°C [41]. At least two types of GBP zones have been distinguished; GPB I, which form immediately following quenching and ageing at temperatures <200°C, and GPB II zones, which form on ageing at higher temperatures (>200-220°C). While these two types of zones exhibit related X-ray diffraction signatures, neither appear to be related structurally to the S' or S phases. Thus, in contrast to the precipitation sequence preceding the formation of θ, it is unlikely that a continuous series of allotropic phase changes precedes the formation of S in ternary Al-Cu-Mg alloys.

The GPB I zones are primarily responsible for the maximum hardness at ageing temperatures <200°C, although the zone structure is increasingly replaced by S' (and S) at higher alloy supersaturations. This accounts for the progressive decrease in maximum hardness observed when alloys are aged at progressively higher temperatures from 130°C to 200°C. However, the maximum hardness at 240°C is almost equal to that at 130°C, and the increase is associated with GPB II zones. In this case, overageing leads to a softening, which is again associated with the replacement of the zone structure by S' and S. This precipitation sequence alone would be expected in those alloys with relatively low Cu:Mg ratios, Figures 6(c),(d). However, in those having higher Cu:Mg ratios, Figures (a),(b), the initial rise in hardness may be due to both GP I and GPB I zones. The GP I zones progress to θ" during the rise to maximum hardness, in the manner described above.

2.2.1. Microalloying: Effects of Ag Additions

The effects of microalloying additions of 0.4 wt% (0.1 at%) Ag on the age-hardening response of Al-Cu-Mg alloys are also shown in Figure 6 (dashed curves), and the increment in hardness that such additions promote is plotted with respect to ageing time at 200°C in Figure 7. The maximum hardness increment that may be achieved with Ag additions is also superimposed in italic on the phase diagram in Figure 5. The quaternary alloys exhibit an accelerated second stage of hardening and a significant increase in maximum hardness compared to the Ag-free alloys of similar composition. As mentioned above, the addition of small concentrations of Ag is known to enhance the age hardening response of all aluminium alloys containing magnesium [3]. Whilst the precise role of silver (and magnesium) remains unclear, a common feature is that silver promotes nucleation of finely-dispersed intermediate precipitates which, in turn, may cause increased strengthening by influencing precipitate/dislocation interactions.

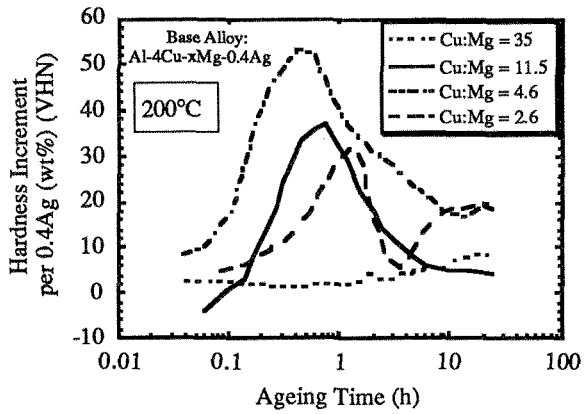

Figure 7. Graph of the hardness increment achieved with microalloying additions of 0.4 wt% Ag to Al-Cu-Mg alloys of varying Cu:Mg ratio. Hardness increment is recorded as a function of ageing time for alloys aged at 200°C. Data from [40].

For Al-Cu-Mg alloys with Cu:Mg ratios sufficiently high that they lie in the (α+θ+S) field of the ternary phase diagram, Figure 5, silver stimulates precipitation of a fine and uniform dispersion of the Ω phase, which forms as thin, hexagonal plates on {111}α planes, Figure 8. It is the Ω phase which promotes greater age hardening in the quaternary alloys in Figures 6(a),(b) [15], and alloys based on

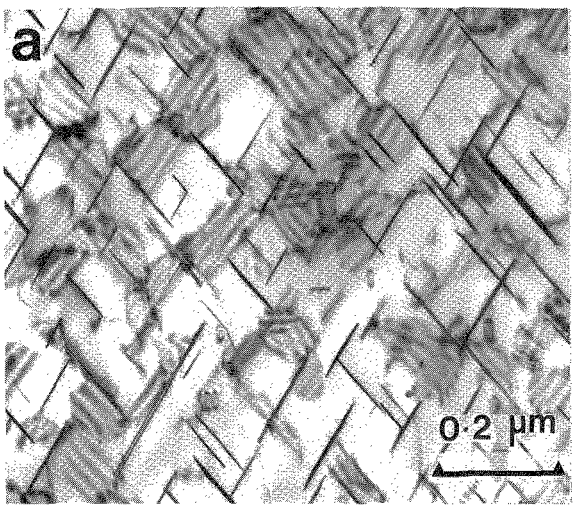

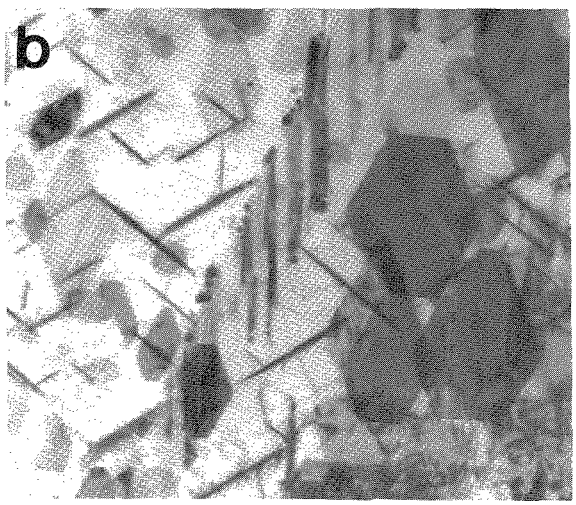

Figure 8. Transmission electron micrographs showing the Ω precipitate phase in an Al-4Cu-0.3Mg-0.4Ag alloy aged 100h at 190°C. The electron beam is parallel to (a) $\langle 110 \rangle_\alpha$, and (b) $\langle 111 \rangle_\alpha$.

the Al-Cu-Mg-Ag system have shown promising creep properties at temperatures up to 200°C because of the relatively high thermal stability of Ω in this temperature range [20]. However, long term ageing (~100 days) of the Al-4Cu-0.3Mg-0.4Ag alloy at the higher temperature of 250°C, Figure 6(b), has shown that the Ω phase is gradually replaced by θ phase

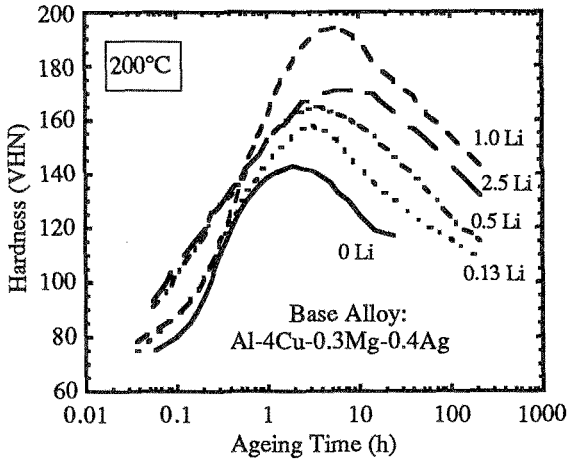

Figure 9. Variation in hardness with ageing time at 200°C for an Al-4Cu-0.3Mg-0.4Ag alloy containing systematic additions of Li. [21].

[42]. For Al-Cu-Mg alloys with lower Cu:Mg ratios such that they lie in the (α+S) field of the ternary phase diagram, Figure 5, silver additions promote precipitation of the T phase, $Al_6(CuAg)Mg_4$, instead of the S' (or S) phases [2,3,13,14] that are otherwise formed. This phase is the dominant precipitate in alloys aged to peak hardness at 200 °C, but it has also proven to be metastable and to transform to the equilibrium S phase on prolonged ageing (e.g. 100 days) [13,14]. It is the T phase which promotes greater hardening in the quaternary alloys in Figures 6(b),(c).

2.2.2. Microalloying: Effect of Cd and Li

Silver additions appear to have little or no effect on the precipitation of the θ' phase in either Al-Cu or Al-Cu-Mg alloys. However, refined dispersions of this phase are promoted by microalloying with Sn, In or Cd, and by somewhat larger additions of lithium [43,44]. On this basis, Polmear and Chester [21] examined the effect of separate additions of Cd and Li on the ageing response of Al-4Cu-0.3Mg-0.4Ag alloy. Although this alloy does not the 7, it the highest response to Ag additions, Figure was selected in the expectation that it would exhibit contain minimal S phase precipitation, Figure 5, leaving the Mg and Ag free to stimulate Ω precipitation in place of θ'. It was found that Cd

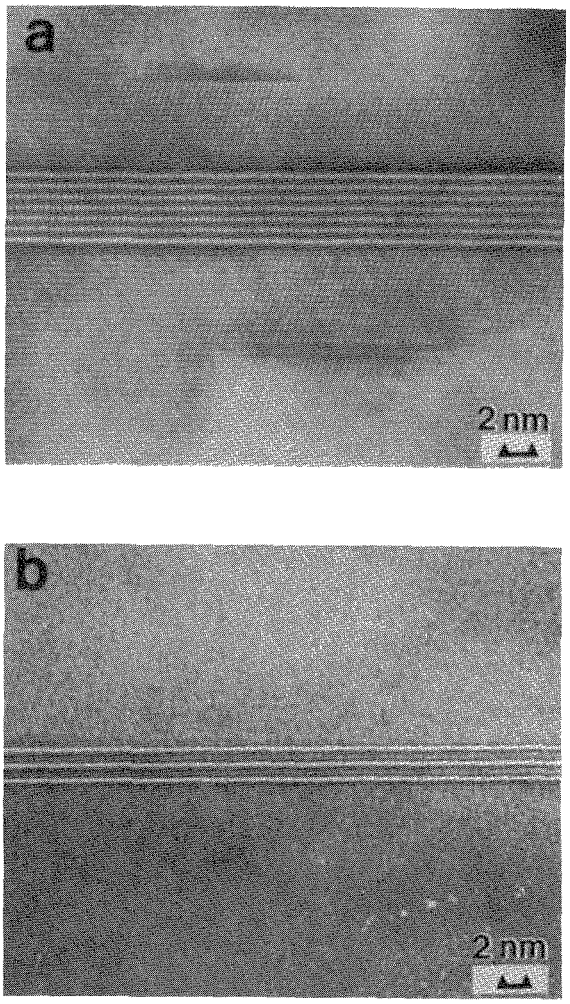

Figure 10. High resolution electron micrographs comparing the structures of (a) Ω phase precipitate in Al-Cu-Mg-Ag alloy, and (b) T_1 phase precipitate in Al-Cu-Li-Mg-Ag alloy (Weldalite 049™). In each case the electron beam is parallel to $\langle 110 \rangle_\alpha$.

had no significant effect on hardening, but progressive additions of Li produced an exceptional age hardening response.

Figure 9 shows hardness curves for an Al-4Cu-0.3Mg-0.4Ag alloy containing systematic Li additions of between 0 and 2.5 wt%, aged at 200°C [21]. An increase in maximum hardness from 143 to 195 VHN is observed with increasing Li content up to ~1 wt%. However, at 2.5 wt% Li, the peak hardness is reduced, suggesting an optimum hardening response at a Li content somewhere between 1.0 and 2.5 wt%. While the base alloy (Al-4Cu-0.3Mg-0.4Ag) is hardened by a fine and uniform dispersion of Ω plates on $\{111\}_\alpha$, and a minor fraction of θ' phase, the addition of as little as 0.13 wt% Li has been reported to reduce the density of $\{111\}_\alpha$ precipitates, promote a finer dispersion of θ' and introduce laths of the S' (or S) phase [21]. Polmear and Chester [21] have suggested that, while the $\{111\}_\alpha$ precipitates remain the primary strengthening constituent, the exceptional hardness of the 1 wt% Li alloy may be attributable to the coexistence of these three effective strengthening precipitates. At higher Li contents (2.5 wt% Li), the principal strengthening precipitate becomes the coherent δ' phase (Al_3Li), which is known to be readily shearable by dislocations [45] and offers less resistance to deformation.

The $\{111\}_\alpha$ precipitates were initially thought to be Ω phase [21], but recent high resolution electron microscopy [24] has indicated that they have a structure similar to that of the T_1 phase, which is the primary intermediate strengthening phase in Al-Cu-Li alloys, Figure 10 [43,46,47]. The T_1 phase forms with some difficulty in ternary Al-Cu-Li alloys during conventional isothermal ageing treatments and, when possible, it is common in commercial practice for such alloys to be deformed plastically prior to ageing (T8 treatment [46,47]) to induce increased heterogeneous nucleation of the T_1 plates and a more uniform precipitate distribution. In those Al-Cu-Li alloys containing microalloying additions of Mg and Ag, these elements have been detected in association with the T_1 plates, and appear, in some way, to facilitate the nucleation of the T_1 phase. It appears likely that it is the fine and uniform distribution of T_1 phase that emerges in the presence of the Mg and Ag that is the main factor in promoting the exceptional strength and hardness of the Al-Cu-Li-Mg-Ag alloys that have emerged as the Weldalite series.

In preliminary results of a systematic study [48] of the effect of Li additions on precipitation behaviour in the Al-Cu-Mg-Ag system, differential scanning calorimetry (DSC) has suggested that the first precipitation reaction that occurs on continuously heating either the Li-free or the Li-containing alloys is the formation of GP zones on

$\{100\}_\alpha$ planes, Figure 11(a). This is followed by the gradual appearance of θ", and then an abrupt precipitation on $\{111\}_\alpha$ planes, Figures 11(b),(c). In all cases, the $\{111\}_\alpha$ precipitates precede the formation of θ', suggesting that the nucleation process for the $\{111\}_\alpha$ precipitates is relatively easy. In those alloys with ~1 wt% Li, the onset of precipitation on $\{111\}_\alpha$ planes is accompanied by the appearance of other phases, which include S' (or S) and which persist even after heating to 350 °C. The early stage ageing aspects of this work in the Li-free alloy have been confirmed by detailed atom probe/field ion microscopy (APFIM) [49].

2.2.3. Microalloying: Effect of Ge and Si

As indicated above, an important effect of trace element additions in Al-Cu alloys is to modify the nucleation and/or growth of the θ' phase, which then replaces the θ" phase at maximum hardness after elevated temperature (130-190°C) ageing. The dense precipitation of trace-modified θ' provides the high strength and hardness in these alloys, whereas θ" is associated with maximum strength in binary Al-Cu alloys, in which overageing and softening follows the formation of coarse and rapidly growing θ'. In an interesting further development, it has been found [50] that Mg interacts strongly in solid solution with both Ge and Si, and that quaternary Al-Cu-Mg-Ge alloys exhibit a much stronger age-hardening response than simple ternary Al-Cu-Mg alloys of similar composition [51]. A smaller but still significant increase in precipitation hardening is also found Al-Cu-Mg-Si alloys. In each case, maximum hardness is associated with fine and uniform dispersions of θ' precipitates. These observations suggest that the stronger the interaction between trace elements, either individually or in combination, and vacancies after quenching, the more rapid is θ' nucleation at elevated temperatures, and the finer and more uniform is the dispersion. It has been proposed [50] that the efficiency of nucleation of θ' increases with trace element additions in the order (Mg+Si),

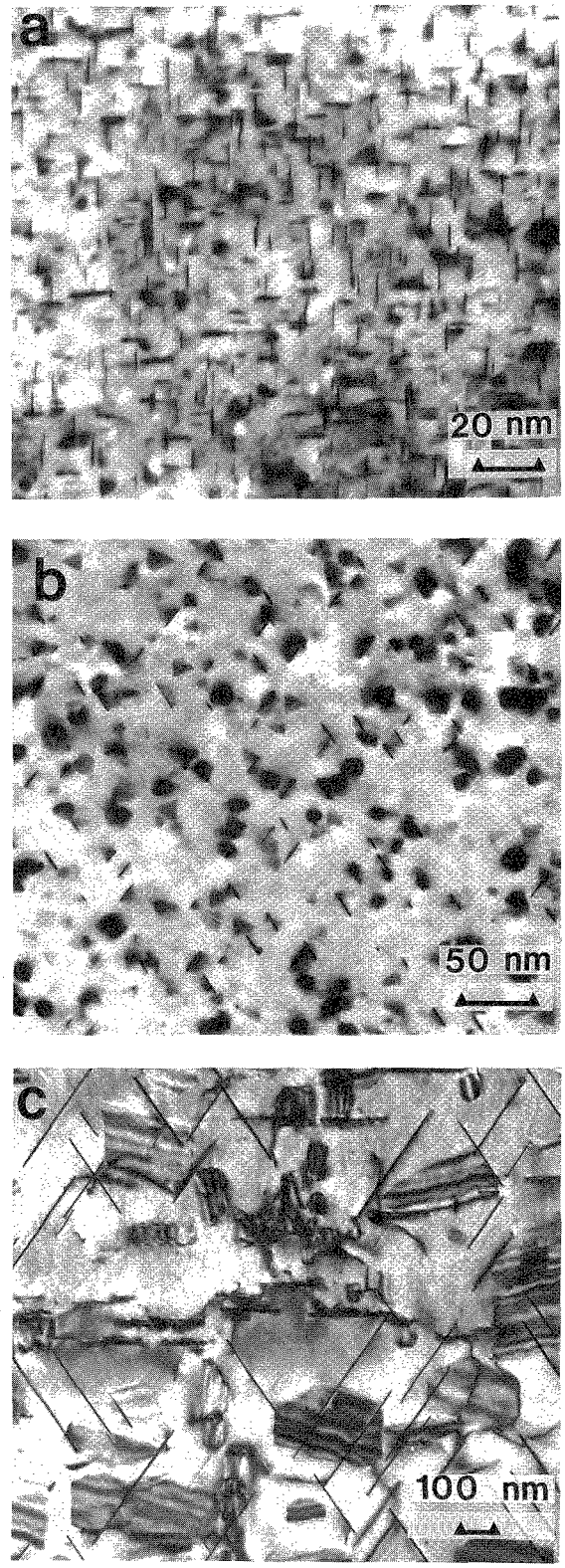

Figure 11. (Adjacent) Transmission electron micrographs from Al-4Cu-0.3Mg-0.4Ag-0.13Li alloy following solution treatment and heating in a differential scanning calorimeter to (a) 175°C, (b) 207°C, and (c) 350°C. The electron beam is parallel to $\langle 001\rangle_\alpha$ in (a), and $\langle 110\rangle_\alpha$ in (b) and (c). [48].

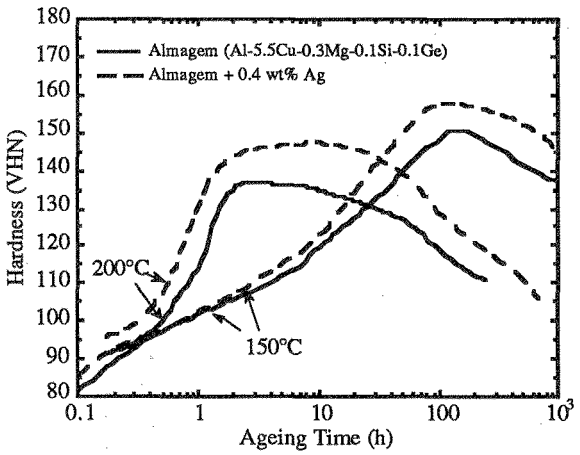

Figure 12. Variation in hardness (VHN) with ageing time at 150°C and 200°C for an Al-Cu-Mg-Si-Ge alloy with and without an addition of 0.4 wt% Ag. [52].

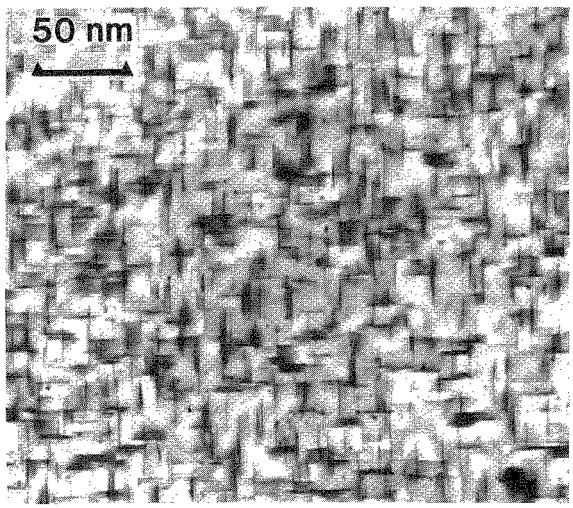

Figure 13. Transmission electron micrograph showing the microstructure of an Al-Cu-Mg-Ag-Si-Ge alloy aged 8h at 150°C. The electron beam is parallel to $\langle 001 \rangle_\alpha$ the dominant precipitate plates are θ' phase and the fine particles are rod-like zones parallel to the electron beam.

Sn (In or Cd), and (Mg+Ge). At the same time, the stability of the resultant θ' dispersion would decrease in the above order. It has been suggested [50] that the increase in θ' stability may be attributable to the segregation of the trace elements, individually or collectively, to the θ'/α interface in such a manner that they retard growth.

These observations provide for a potential approach to rational alloy design, using different trace elements to achieve specific properties. For example, Ge might be used to partially replace Si to accelerate and refine the θ' precipitation, whilst maintaining the high thermal stability characteristic of (Mg+Si) modified alloys. Alternatively, the (partial) replacement of Ge by Si might be used to promote GP zone formation at ambient temperatures, thus introducing a natural ageing response for the alloy, which might be desireable, for example, following welding.

In a further interesting example of the effects of multiple trace element additions, recent characterisation [52] of an Al-Cu-Mg-Ag alloy containing microalloying additions of Si, Ge (and Zr) has revealed that, in the presence of small concentrations of Si and/or Ge, Ag has much less of an effect on the age hardening response. Figure 12 shows a comparison of the hardness curves obtained for an Al-Cu-Mg-Si-Ge alloy with and without Ag additions and indicates that, while there is a systematic increase in the hardness of the Ag-containing alloy, the difference between the Ag-free and Ag-containing alloys is modest. While a quaternary Al-Cu-Mg-Ag alloy contains predominantly Ω phase at maximum hardness, the alloy with Si and/or Ge additions is strengthened by a combination of rod-like (Cu,Mg) zones and θ' phase, Figure 13, up to maximum hardness, irrespective of whether the alloy contains Ag or not. The presence of Si and Ge appears to favour the formation of the rod-like zones during the early stages of ageing, exhausting the supply of Mg and thus preventing the formation of the Ω phase that is characteristic of the quaternary alloy.

3. THE Al-Zn-Mg SYSTEM

3.1. Ternary Al-Zn-Mg Alloys

Alloys based on the Al-Zn-Mg system are generally regarded as having the highest response to

age hardening of all aluminium alloys. They possess lower densities than Al-Cu based alloys, and the combined strength and weight advantage has allowed alloys based on this system to remain very competitive in the development of new aerospace materials. A drawback to the use of these alloys has been their inherent susceptibility to stress corrosion cracking (SCC) . A massive research effort over the last half century has been devoted to reducing this susceptibility, and significant progress has been made [53]. However, the full capability of the alloy system has not yet been exploited and alloys with high Zn and Mg levels, which demonstrate very high strengths have yet to be used safely.

Figure 14 shows the Al-rich corner of the ternary phase diagram at 200°C. The phase boundaries are not thought to change significantly down to as low as room temperature [54]. A feature of the diagram is the wide range of composition of the (α+T) phase field, which contains most of the alloy compositions of commercial significance. The T phase is a ternary intermetallic compound, with stoichiometry $(Al,Zn)_{49}Mg_{32}$, whilst the η phase is a binary intermetallic of composition $MgZn_2$. While these represent the equilibrium phases in the ternary system, the strong age-hardening response and maximum hardness are commonly associated with metastable intermediate forms of the η phase, most notably that designated η'. Typical values of tensile strength achievable in this system are superimposed on Figure 14, where the thin dashed lines represent ultimate tensile strength and the thin solid lines represent the tensile yield strength as a function of composition. This compilation of data [53] shows strength values (MPa), which range from 450-600 MPa, with the highest tensile strengths being recorded for alloys with high Zn and Mg levels. The thick dashed lines labelled Mg and Zn represent the minimum level of each individual alloying addition that will give a high response to age hardening (maximum hardness >140VHN) as a function of alloy composition.

The strong empirical basis to the development of this alloy system has created a situation where, even now, much remains unclear about the mechanisms behind the age hardening behaviour. Extensive work by Polmear and co-workers [12,55-58] suggests that the phases formed depend more on the temperature of ageing than the position of the alloy in the phase diagram. Furthermore, the ageing processes appear similar for a wide range of alloy compositions. Figures 15(a-d) show typical age-hardening curves for several Al-Zn-Mg alloys. It is widely accepted that hardening is associated with a precipitation sequence involving the initial decomposition of supersaturated α solid solution to GP zones, which may transform in-situ to a metastable intermediate precipitate, followed by a transition to the final equilibrium precipitate phase or phases. At the lower temperatures, the formation of GP zones is spontaneous, but on ageing above a critical temperature there emerges an apparent barrier to nucleation resulting in a heterogeneous dispersion of GP zones on lattice defects, particularly dislocation loops [53,59]. This critical temperature or upper temperature limit for spontaneous GP zone formation varies with alloy composition and lies typically between 90 and 180°C [55].

It is thought that the GP zones comprise spherical or ellipsoidal clusters of Mg and Zn atoms, which form on the matrix $\{111\}_\alpha$ planes [53,60-62]. The zone size is initially 0.5-1.0 nm, but grows rapidly to a maximum of 5-15 nm after prolonged ageing. The GP zone size seems to be independent ofageing temperature and this is thought to be controlled by coherency strains [59,63]. It is these GP zones that are responsible for the initial rise in hardness shown in Figure 15. The incubation of these zones is more prominent at lower temperatures, leading to a pronounced hardness plateau and a very fine zone dispersion. The second stage of hardening occurs on ageing in the range 100-200°C and is associated with the formation of the intermediate phase η', Figure 16. There remains some uncertainty about the step from the GP zones to η', although it is widely acknowledged that the zones are intimately associated with the nucleation of η'. Disagreement remains as to whether the zones act as potent nucleation sites or whether more favorable local conditions surrounding certain zones causes them to undergo an ordering reaction and transform to the intermediate phase. The structure and detailed ageing behaviour of this important phase (η') remain unclear; however, a hexagonal structure similar to the equilibrium η phase ($MgZn_2$), but with slightly different lattice parameters, is the most commonly reported [64-66]. This phase may exist in a variety of orientations and morphologies and its presence,

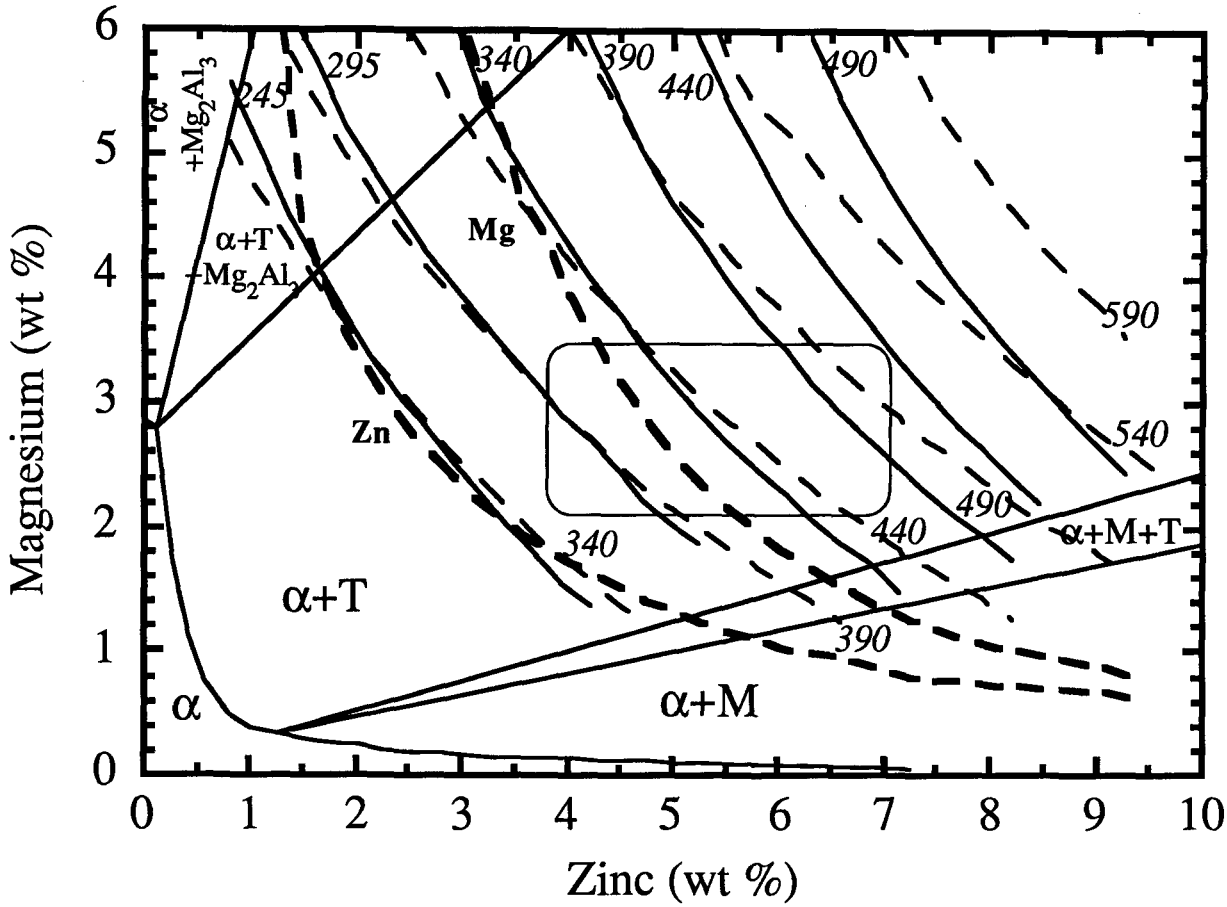

Figure 14. Aluminium-rich corner of the Al-Mg-Zn ternary phase diagram at 200°C. Diagram contains superimposed contours of constant yield strength (solid curves) and ultimate tensile strength (UTS) (thin dashed curves) attainable as a function of alloy composition. Thick dashed curves define lower limits of Zn and Mg contents of alloys with high age hardening response (maximum hardness >140 VHN). Frame insert defines composition range for common commercial alloys. [53-58]

sometimes togetner with GP zones from the initial stages of hardening, is responsible for maximum hardness, Figure 15.

The most significant age hardening occurs at 120°C, where it is thought that a fine and uniform GP zone dispersion develops during the first stage of ageing. At the higher (8 wt%) Zn level, the first stage of hardening is more rapid and GP zone incubation times less, resulting in a less prominent hardness plateau. A similar mechanism is considered to operate in all of the ternary hardening curves in Figure 15, with the degree of supersaturation modifying the size and dispersion of GP-zones, but not thought to cause a phase change. The third stage of ageing in these alloys involves the formation of the equilibrium phases. Here also, fairly general behaviour holds over a wide range of conditions and it is only when ageing is carried out above 200°C that the position of the alloy in the phase diagram appears to influence the identity of the precipitate formed. Below 200°C, η phase results, whilst above this temperature, η' replaces the GP zones in the first to retard the formation of GP zones, as the ternary trace-modified alloys are observed to age harden more stage of ageing and η transforms to T phase if the alloy lies in the (α+T) phase field, Figure 14.

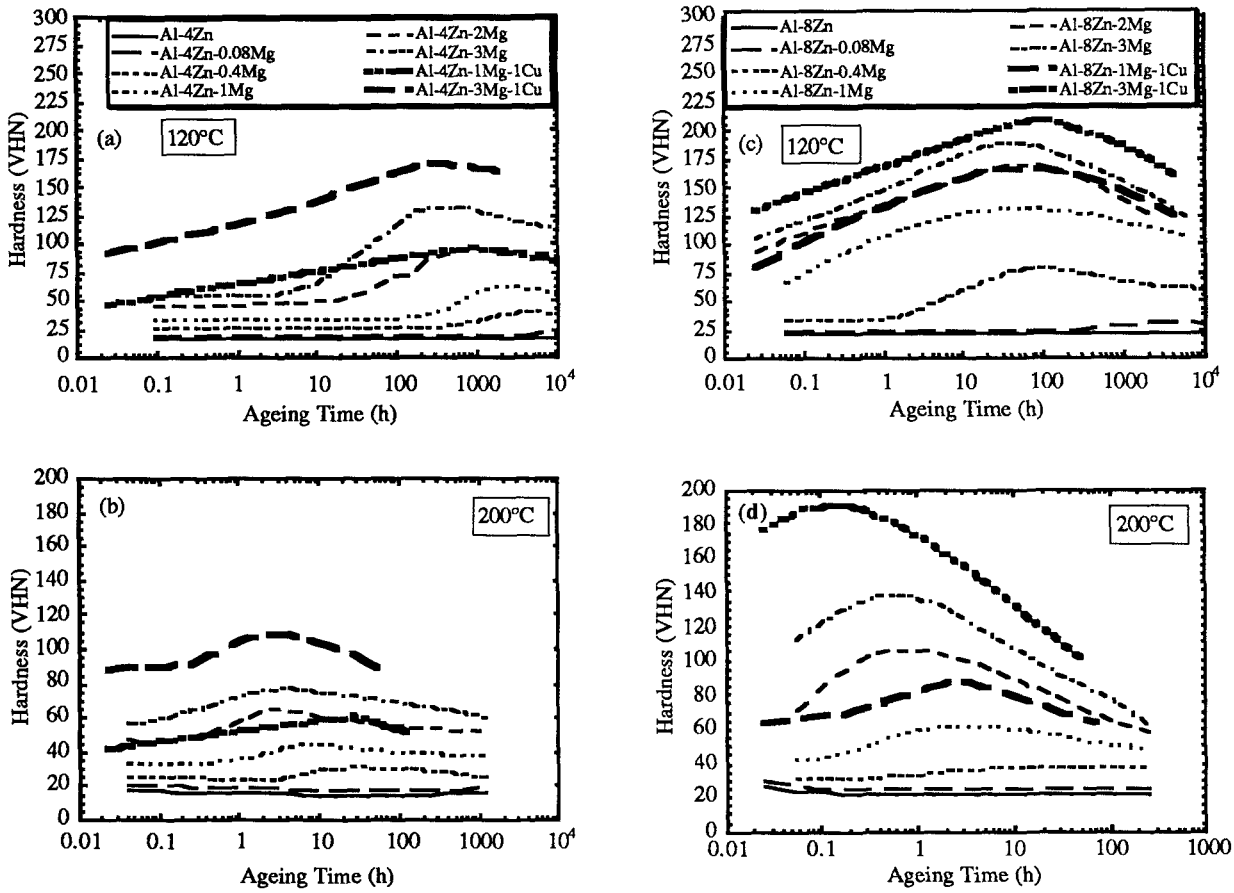

Figure 15(a-d). Variation in hardness (VHN) with ageing time at 120°C and 200°C for a range of Al-Zn-Mg(-Cu) alloys.

3.2. Microalloying: Cu and Ag

The addition of Cu to Al-Zn-Mg alloys causes a significant improvement in resistance to SCC. This has been attributed to a reduction in the electrode potential difference between grains and grain boundaries [67] and the fact that Cu seems to reduce the susceptibility to intergranular weakness [68]. Both of these effects are due to the way Cu influences the precipitation reactions in these alloys and, in particular, the early stages of hardening. For ageing in the range 100-235°C, very rapid hardening occurs in the initial stages, Figure 15, indicating that a phenomenon distinct from the basic ageing processes of the ternary alloys is occurring. There has been some suggestion that this is due to the formation of the S phase (Al_2CuMg) [11]. With regard to peak hardness, however, the effect of Cu is similar to that obtained from an equivalent amount of Zn [53], and this is well envisaged from the hardening curves in Figure 15. It is considered that Cu has little effect on the second stage of ageing and there is a variety of experimental evidence that supports the notion that once the first stage of hardening is completed, the Cu-bearing quaternary alloys age-harden in the same way as the equivalent ternary alloys [11].

The addition of Ag to Al-Zn-Mg alloys can stimulate an enhanced response to age hardening in a manner similar to its effects in Al-Cu-Mg alloys.

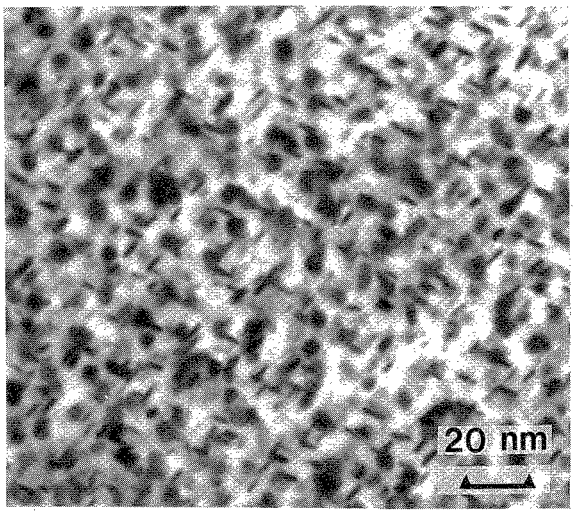

Figure 16. Transmission electron micrograph showing platelets of η' phase on $\{111\}_\alpha$ planes in Al-8Zn-2Mg-0.5Ag alloy aged 2 h at 150°C. The electron beam is parallel to $\langle 110\rangle_\alpha$. (Micrograph courtesy Y.-S. Lee).

Figure 17 represents the Al-rich corner of the Al-Zn-Mg phase diagram and shows contours representing constant increments in hardness that may be achieved with the addition of 0.5 wt% Ag. This construction assumes solution treatment has been performed at 460°C and the increment represents the maximum achievable at typical artificial ageing temperatures. The diagram is taken from the work of Vietz et al [58] and shows that the response of Al-Zn-Mg alloys to Ag additions does not appear to be controlled by the position of the alloy in the phase diagram. It has been suggested that the maximum hardening response occurs when Ag is added to compositions for which the product [Zn] x [Mg] = 8.5 (wt%).

It has been found that a critical concentration of Ag is required to stimulate the effect and that this critical concentration increases with increasing ageing temperature. As with the hardening associated with Ag additions to Al-Cu-Mg alloys, the mechanism behind the increased hardening response in this case is not well understood, but may be associated with an increase in the upper temperature limit of stability of GP zones. There is an accumulation of metallographic evidence, however, that suggests Ag somehow stimulates the nucleation of a fine and uniform dispersion of η'.

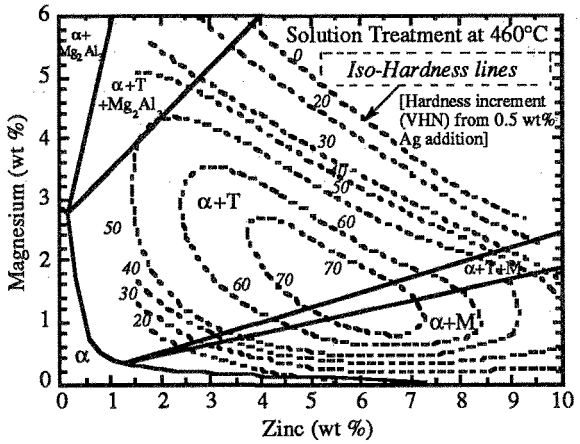

Figure 17. Aluminium-rich corner of the Al-Zn-Mg ternary phase diagram at 200°C. Superimposed are contours of constant hardness defining the hardness increment (VHN) that may be attained with a Ag addition of 0.5 wt%. [58].

Again, an interaction between vacancies, Mg and Ag atoms is proposed to be responsible for this effect [11,55-58]. The addition of Ag allows high hardening/strength levels in alloys having lower Zn and Mg contents and represents a novel approach to the problem of SCC in these high strength alloys. Not only are lower Zn and Mg containing alloys less susceptible to SCC, but the Ag additions promote such uniform precipitation that particle free zones adjacent to grain boundaries, linked to the onset of SCC, are essentially eliminated.

3.3. Commercial Alloys

The 7XXX series of Al-Zn-Mg alloys are generally amongst the highest strength wrought Al-alloys available. They can be divided into two categories; those which do not contain Cu and those which do. The Cu free alloys represent medium strength materials, which are readily weldable. They harden considerably at room temperature allowing excellent recovery of mechanical properties in the heat affected zone following welding, and welded components usually have tensile yield strength properties superior to those of Al-Mg and Al-Mg-Si alloys [1]. Commercial alloys often contain Mn and/or Cr since a significant improvement in the stress corrosion resistance is found. Additions of Zr are also common as these also allow recrystallization

to be inhibited, and provide for stability of the cold worked structure. Whilst the addition of Cu has significant influence on the strength of the alloy and a profound improvement in the SCC resistance, the weldability does suffer and Cu levels must typically be below 0.3 wt% if welding is desired, so as to minimize the risk of hot cracking during weld solidification. The use of microalloying additions of Ag as a method of reducing SCC is presently regarded as too great a cost penalty to support wide commercial application.

4. THE ROLE OF $\{111\}_\alpha$ PRECIPITATES

It is interesting to note that there are marked similarities in the structure and mode of formation of those precipitate phases known to promote high strength in the alloys of interest. Of prime concern are the Ω phase formed in Al-Cu-Mg and Al-Cu-Mg-Ag alloys (Figure 8), the T_1 phase (Al_2CuLi) which forms in the Al-Cu-Li alloys (Figure 11), and the η' phase present as an intermediate phase in Al-Zn-Mg(-Cu) and Al-Zn-Mg-Ag alloys at maximum hardness (Figure 16). All three phases form as hexagonal-shaped plates or platelets on the $\{111\}_\alpha$ planes in an aluminium matrix. The determination of the crystal structures of all three has proven controversial. Initial studies of the structure of the Ω phase suggested, for example, that it was either monoclinic (a =b = 0.496 nm, c = 0.848 nm, γ = 120°) [16] or hexagonal (a = 0.496 nm, c = 0.701 nm) [69]. However, recent work [17,18] has provided strong experimental support for the conclusion that it is in fact orthorhombic (Fmmm, a = 0.496 nm, b = 0.859 nm, c = 0.848 nm). In each of these studies it has been recognised that the structure of Ω also bears a close relationship to that of the equilibrium, tetragonal phase θ (I4/mcm, a = b = 0.6066 nm, c = 0.4874 nm), which forms on ageing binary Al-Cu alloys at high temperatures, and in some recent work [70] the Ω phase has been identified as representing a certain crystallographic variant of θ. Garg and Howe [71] have also recently reported the presence of a tetragonal phase (point group 4/mmm, a = b = 0.6066 nm, c = 0.496 nm), designated θ_m, in an Al-4Cu-0.5Mg-0.5Ag (wt%) alloy aged at the high temperatures of 250°C and 350°C. However, since these observations were made during in-situ ageing of thin foils in the hot stage of a transmission electron microscope (TEM), the behaviour may not be typical of the bulk alloy, and the significance of the θ_m phase remains to be resolved.

The roles of Mg and Ag in stimulating the formation of the Ω phase in Al-Cu alloys are not yet fully understood. Independent investigations using energy dispersive x-ray spectroscopy [18] and atom probe field ion microscopy (APFIM) [49] have established that the Mg and Ag partition to the Ω phase from the earliest stages of plate formation that can be readily detected, and have suggested that these elements segregate to the interface between the Ω phase and the α matrix. Recent detailed studies [72] of the very early stages of ageing in an Al-Cu-Mg-Ag alloy using APFIM have revealed that, in the solution treated and quenched condition, the microstructure contains independent clusters of Cu, Mg and Ag atoms. After ageing for 15 sec. at 180°C, the Mg and Ag are detected in combination, and with a further 15 sec. at 180°C, co-clustering of Mg, Ag and Cu atoms is evident. Coinciding with the detection of the (Mg,Ag,Cu) atom clusters in the APFIM, extremely small precipitates, believed to be the precursor to the formation of the Ω phase, become detectable using transmission electron microscopy. However, the relationship between the pre-precipitate clustering and the development of the $\{111\}_\alpha$ precipitates is yet to be firmly established.

A number of studies of the T_1 phase have identified a hexagonal structure (a = 0.496 nm, c = 0.935 nm) [24]. However, there remains disagreement as to the origin of additional reflections observed in selected area electron diffraction patterns from the phase [24,47]. Given that the structure of the Ω phase is based on a hexagonal lattice, the Ω and T_1 lattices differ significantly only in the lattice dimension normal to the basal plane (c axis), which is parallel to the precipitate habit plane. In the case of Ω phase plates, the plate thickness is restricted by a large misfit (~9.3%) in interatomic spacing along directions normal to the habit plane in precipitate and matrix. However, in the case of T_1 plates the c dimension is almost exactly four times the $\{111\}_\alpha$ interplanar spacing and it is not clear why the growth of such plates normal to the habit plane remains restricted [47].

The η' phase is reported to be a transition stage in the formation of the η phase ($MgZn_2$) in quenched

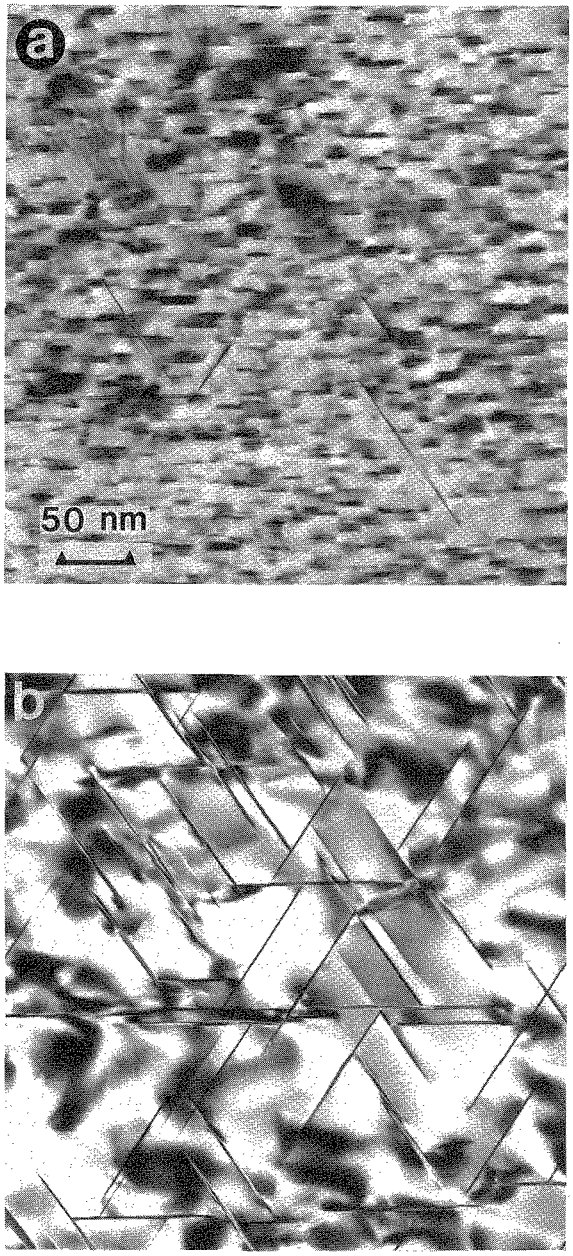

Figure 18. Transmission electron micrographs of an Al-5.3Cu-1.3Li-0.4Mg-0.4Ag-0.14Zr alloy comparing (a) quenched and aged 8h at 160°C with GP zones and sparse T_1 plates (hardness 146 VHN) and (b) quenched, cold rolled and aged 8h at 160°C with a uniform distribution of T_1 plates (hardness 200 VHN).

and aged Al-Zn-Mg alloys, with maximum hardness being attributable to a combination of the GP (Zn,Mg) zones and a coarser dispersion of the semi-coherent η'. Microalloying additions of Ag enhance hardening by promoting a fine and uniform dispersion of η', although the precise role of Ag is uncertain. The η' phase has received less recent attention, but has also been the subject of controversy. It has been reported as either hexagonal (a = 0.496 nm, c = 0.868 nm) [64,65] or monoclinic (a = b = 0.497 nm, c = 0.554 nm, γ = 120°) [66] and, in either case, is thus equivalent in the a parameter to Ω and T_1, but again different in the c parameter. Based on lattice dimensions, all three $\{111\}_\alpha$ precipitate phases would appear to be almost perfectly coherent with the aluminium matrix within the $(111)_\alpha$ habit plane, which is the basal plane for the hexagonal T_1 and η' phases, and the (001) plane for the orthorhombic Ω. The T_1 and Ω phases are able to grow extensively parallel to the habit plane to establish plates of remarkably large aspect ratio (e.g. 200:1), by what appear to be similar growth mechanisms involving the passage of Shockley partial transformation dislocations across the broad faces of the plates [19,39,46,47]. However, the η' phase remains restricted to platelets typically less than 20 nm in diameter, with an aspect ratio of approximately 5:1 [73]. The origin of this comparative constraint to the growth of η' plates in the habit plane remains to be properly understood.

An additional important feature of these alloys worthy of further study is the effect that plastic deformation, applied prior to the ageing treatment, has on the precipitate distribution and thus strength. In Al-Cu-Li alloys strengthened by the T_1 phase, maximum strength is commonly achieved by incorporating a tensile plastic deformation of typically 3-6% prior to ageing (T8 temper) [46]. Nucleation of the T_1 phase is apparently stimulated strongly by an increase in the dislocation density in the matrix phase, despite the fact that the T_1 plates are coherent with the α matrix in the precipitate habit plane and have only a small misfit strain (~0.12%) normal to the habit plane [24,47]. No similar response has been observed in Al-Cu-Mg-Ag alloys strengthened by the Ω phase, despite the fact that the Ω plates accumulate a misfit of ~9.3% perpendicular to the $\{111\}_\alpha$ habit plane [74]. There is currently no completely satisfactory explanation of

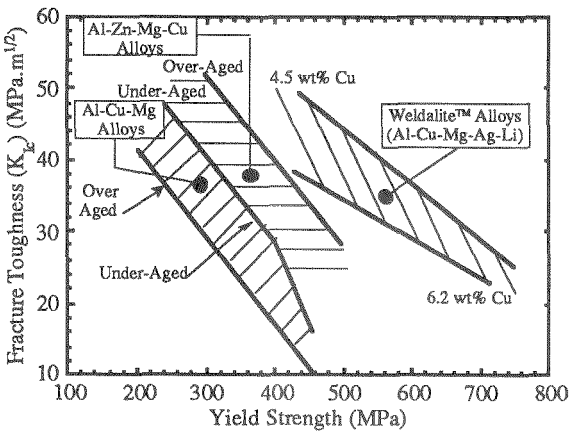

Figure 19. Comparison of fracture toughness ranges (K_{Ic}) observed for selected high to ultra-high strength aluminium alloys. [22, 81]

the response of the T_1 phase to prior plastic deformation and the differences in behaviour of the T_1 and Ω phases in these circumstances. In Al-Cu-Mg-Ag alloys containing Li, recent work has established that prior plastic strain accelerates precipitation of the $\{111\}_\alpha$ precipitates [74,75], which is consistent with accumulating evidence that these precipitates are predominantly T_1 phase or T_1-like, Figure 10 [24]. Figure 18 shows transmission electron micrographs of an Al-5.3Cu-1.3Li 0.4Mg-0.4Ag-0.16Zr alloy (a) quenched and aged 8h at 160°C, and (b) quenched, cold-rolled 6% and aged 8h at 160°C. The prior plastic deformation promotes an increased density and uniform dispersion of T_1 plates, and a corresponding increase in hardness for equivalent ageing treatments. However, prior plastic deformation produces little significant increase in the maximum strength of the Li-containing alloys.

The role of the trace additions of Mg and Ag in Al-Cu-Li alloys such as Weldalite 049™ appears to be to stimulate the formation of the T_1 phase or a T_1-like phase, and thus eliminate the need for the deformation step that is common in the processing of ternary Al-Cu-Li alloys. The resulting alloys enjoy a substantial strength advantage over ternary Al-Cu-Li alloys and Al-Cu-Mg-Ag alloys, and there remains a need for systematic work to characterize the effects of prior plastic deformation on precipitate distributions in these alloys and to examine the deformation characteristics and strengthening mechanisms in those alloys subjected to deformation prior to ageing. These observations also reinforce the need for further study of the strengthening mechanisms in the Li-containing Al-Cu-Mg-Ag alloys to establish whether the exceptional strength that they exhibit is attributable to the identity and distribution of an individual precipitate phase (i.e T_1) or to the presence of a critical mix of different precipitate phases and perhaps other factors.

5. TOWARDS AN ULTRA-HIGH STRENGTH ALUMINIUM ALLOY

The comparison of tensile properties of selectedhigh strength aluminium alloys shown in Table 1 demonstrates clearly that microalloying additions of Mg and Ag to Al-Cu alloys produces a substantial increase in alloy strength. The developmental quaternary Al-Cu-Mg-Ag alloy [20] has a yield strength in excess of 500 MPa, compared to a typical maximum of 350 MPa for the existing commercial structural alloy 2219 in the T8 temper, and this advantage is sustained whilst retaining a tensile elongation equivalent to the 'binary' alloy (~5-10%). When an addition of approximately 1 wt% Li is made to the quaternary alloy, there is a further remarkable increase in yield strength to in excess of 700 MPa with appropriate processing. The emerging Weldalite 049™ series of alloys [22] based on this quinary composition offer the prospect of being the first aluminium alloys to be equivalent to ultra-high strength steels (tensile properties above 2100 MPa) on the basis of strength:weight ratios. Both the Li-free and the Li-containing microalloyed Al-Cu alloys have proven to be weldable, and both retain useful ductility (7-9 % tensile elongation) and toughness at these high strength levels. Figure 19 includes fracture toughness data for the Weldalite 049™ series of alloys and demonstrates that the alloys compare favourably with existing high strength Al-Cu-Mg and Al-Zn-Mg-Cu alloys. For tensile yield strengths in the range 600 to 700 MPa, the Weldalite alloys are capable of a fracture toughness typically of the order of 30 MPa.m$^{1/2}$.

A further impressive feature of the performance of these alloys is the thermal stability of the precipitate structures that confer their strength, and the improved

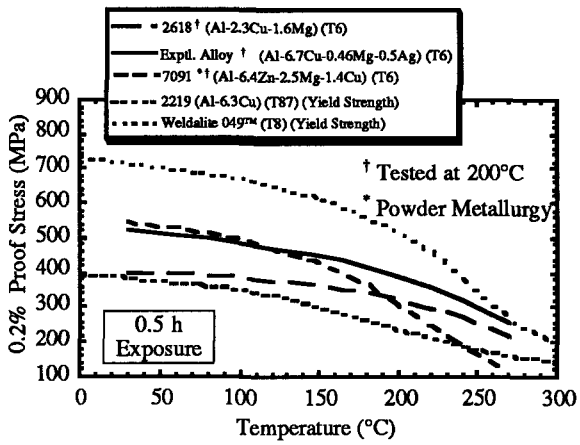

Figure 20. Variation in the 0.2% proof stress with temperature after 0.5 h exposure to elevated temperature for selected high and ultra-high strength aluminium alloys. [20].

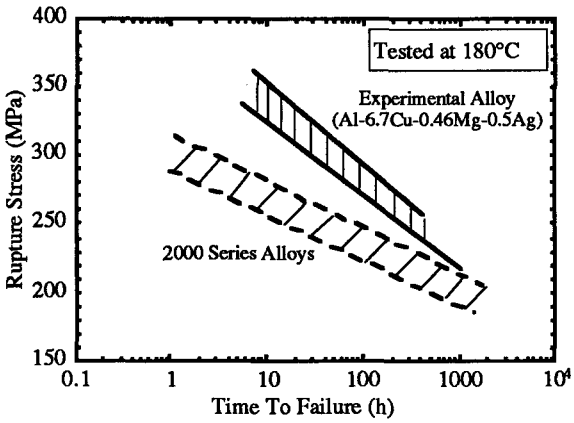

Figure 21. Comparison of creep rupture properties of experimental Al-Cu-Mg-Ag alloy with those of conventional 2000 series Al-Cu based alloys. Diagram shows time to failure (h) at a given rupture stress (MPa) for tests conducted at 180°C [20].

high temperature strength and creep properties that arise from this stability. As illustrated in Figure 4(a), the yield strength of conventional medium to high strength alloys decreases rapidly with testing temperature at temperatures above approximately 100 - 150°C. However, the developmental Al-Cu-Mg-Ag alloy exhibits superior high temperature strength when compared with existing advanced Al-Cu, Al-Cu-Mg and Al-Zn-Mg-Cu alloys, Figure 20. The yield strength of the microalloyed quaternary alloy at 200°C remains above 400 MPa (following 0.5 h exposure at 200°C), reflecting the observed thermal stability and resistance to coarsening of the Ω phase at temperatures up to 200°C [20,76]. As a further indication of the improvement in high temperature properties exhibited by the microalloyed alloy, Figure 21 compares the creep properties of the experimental alloy with those of existing commercial 2000 series Al-Cu based alloys. The data indicate that the time to failure at a given level of applied stress is increased significantly for the experimental alloy at all stress levels above ~200 MPa, and that the extent of the improvement increases with increasing stress level to be an order of magnitude difference at 300 MPa.

The Li-containing, microalloyed alloy (Weldalite 049™) enjoys a substantial advantage in strength over the Li-free alloy when tested at ambient temperature and this improvement is largely sustained to temperatures in excess of 200°C. After 0.5 h exposure at 200°C, the yield strength of the Weldalite 049™ alloy measured at that temperature remains in excess of 550MPa.

In common in this important class of alloys, the high tensile yield strength (500-750 MPa) and thermal stability is attributable to precipitation strengthening associated predominantly with the formation of very fine-scale, plate-shaped precipitates, forming on either $\{100\}_\alpha$ or $\{111\}_\alpha$ planes of the α-Al matrix phase [1]. Despite the significance of the alloys as a group, there is currently little detailed quantitative understanding of the strengthening mechanisms operative and the relationship between the form and distribution of the strengthening precipitate phases and the observed tensile strength. Structural alloy development remains largely empirical and, although there have been recent concerted efforts [77,78] to establish an improved theoretical basis for alloy design, such attempts are inevitably limited by a lack of reliable experimental observations of deformation mechanisms in the systems of interest. Although the major strengthening precipitates are invariably plate-shaped with rational crystallographic habit planes and very large aspect ratios, current theories of

strengthening [7,8] are based on randomly distributed, three-dimensional particles characterized by an 'effective diameter', which is commonly assumed to be the plate thickness [78]. Little or no attention is given to the structure, form, orientation and distribution of the precipitates, although a detailed quantitative understanding of the roles of these factors is essential to the prediction and control of the required microstructures.

The exceptional strength of the Weldalite series of alloys has been attributed [21,24] to an effective uniform, fine-scale distribution of T_1 phase plates, promoted by microalloying additions of Mg and Ag, combined with contributions from the simultaneous presence of θ' and S phases. However, plausible as this proposal may be, it is a difficult proposition to evaluate because of the current lack of understanding of the factors important in defining the strength of this group of alloys. While the Li-containing Al-Cu-Mg-Ag alloys appear superior in strength to Li-free alloys, it is not clear, for example, whether this might be attributable to

(i) intrinsic differences in the effectiveness of the primary strengthening phases T_1 and Ω respectively,

(ii) differences in the scale and distribution of precipitates in the two alloys,

(iii) differences in the mix of precipitates formed in the two systems at maximum strength, or to

(iv) some combination of these (and perhaps other) factors.

While the T_1 and Ω phases both form as thin plates on $\{111\}_\alpha$ and are virtually perfectly coherent with the surrounding α-Al matrix phase in the habit plane [18,19,47], they are structurally distinct and differ significantly in the degree of misfit that they sustain with the matrix phase normal to the habit plane. It remains to be established whether this may be an important factor in determining the intrinsic resistance of the precipitates to shearing. The intermediate precipitate phases of major interest T_1, Ω, θ' and S' are all commonly described as being resistant to shearing [78], but there is now clear preliminary evidence [47] that T_1 plates of a scale common to peak strength microstructures (typically 50 nm thickness) in Al-Cu-Li alloys may be readily sheared by gliding dislocations. It again remains to be established whether there is some critical thickness at which such plates become resistant to shearing, whether this thickness corresponds to maximum hardness of the alloys, whether it remains appropriate to regard the T_1 plates as 'non-shearable' and thus whether existing experimental observations can be reconciled with current theories of precipitation strengthening. Such work needs to be extended to other $\{111\}_\alpha$ precipitates which have and similar form to the T_1 phase, but differ in structure and degree of misfit normal to the habit plane (e.g. Ω the metastable γ' phase in Al-Ag alloys [79]), and to other metastable, intermediate precipitate phases that have different crystal habits.

REFERENCES

1. I.J. Polmear, 'Light Alloys: Metallurgy of the Light Metals', Edward Arnold, 2nd Edition, (1989) 278.
2. I.J. Polmear, Proc. 3rd Intl. Conf. on Aluminium Alloys (ICAA-3), (L. Arnberg, O. Lohne, E. Nes and N. Ryum, eds.), NTH-SINTEF, Trondheim, Norway, Vol. III, (1992) 371-84.
3. I.J. Polmear, Mater. Sci. Forum, Vol. 13/14, (1987) 195-214.
4. A.K. Mukhopadhyay, G.J. Shiflet and E.S. Starke, Morris E. Fine Symposium, (P.K. Liaw, J.R. Weertman, H.L. Marcus and J.S. Santner, eds.), TMS-AIME, Warrendale, PA, (1991) 283-291.
5. T. Gladman, D. Dulieu and I. D. McIvor, Microalloying '75, Intl. Symp. on High Strength Low Alloy Steels, Union Carbide Corp., Washington, (1975) 25.
6. I.J. Polmear, Proc. 10th Risø Int. Symp. on Metallurgy and Mater. Sci., Materials Architecture, (J.B. Bild Sorensen, N. Hansen, D. Juul Jensen, T. Leffers, H. Liholt and O.B. Pederson, eds.), Risø National Lab., Roskilde, Denmark, (1989) 521.
7. E.A. Starke Jr., in 'Aluminium Alloys Contemporary Research and Applications', Treatise on Materials Science and Technology, Vol. 31, (A.K. Vasudevan and R.D. Doherty,eds.) , Academic Press, (1989) 35-63.
8. J.D. Embury, D.J. Lloyd and T.R. Ramachandran, ibid., (1989) 579-601.
9. H.K. Hardy, J. Inst. Metals, Vol. 80, (1952) 483-92.

10. I.J. Polmear and H.K. Hardy, ibid., Vol. 81, (1953) 427-31, .
11. I.J. Polmear, J. Inst. Metals, Vol. 89, (1960) 51-59.
12. I.J. Polmear, Trans. Met. Soc. AIME, Vol. 230, (1964) 1331-39.
13. J.H. Auld, J.T. Vietz and I.J. Polmear, Nature, Vol. 209, (1966) 703-4.
14. J.T. Vietz and I.J. Polmear, J. Inst. Metals, Vol. 94, (1966) 410-19.
15. J.H. Auld and J.T. Vietz, in The Mechanism of Phase Transformations in Crystalline Solids, Inst. of Metals, London, Monograph and Report Series, No. 33, (1969) 77-79.
16. J.H. Auld, Acta Crystall., Vol. 28A, (1972) 98.
17. K.M. Knowles and W.M. Stobbs, Acta Crystall., Vol. B44, (1988) 207-27.
18. B.C. Muddle and I.J. Polmear, Acta Metall., Vol. 37, (1989) 777-89.
19. A. Garg and J.M. Howe, Acta Metall. Mater., Vol. 39, (1991) 1939.
20. I.J. Polmear and M.J. Couper, Metall. Trans. A, Vol. 19A, (1988) 1027-35.
21. I.J. Polmear and R.J. Chester, Scripta Metall., Vol. 23, (1989) 1213-17.
22. J.R. Pickens, F.H. Heubaum, T.J. Langan and L.S. Kramer, Proc. 5th Int. Conf. on Aluminium-Lithium Alloys, (E.A. Starke and T.H. Sanders, eds.), Mat. and Comp. Eng. Publications, Birmingham, U.K., (1989) 1397-1414.
23. F.W. Gayle, F.H. Heubaum and J.R. Pickens, Scripta Metall. Mater, Vol. 24, (1990) 79-84.
24. R.A. Herring, F.W. Gayle and J.R. Pickens, J. Mater. Sci., Vol. 28, (1993) 69-73.
25. G.W. Lorimer, in 'Precipitation Processes in Solids', (K.C. Russell and H.I. Aaronson, eds.), TMS-AIME, Ch. 3, 1978.
26. A. Guinier, Nature, Vol. 142, (1939) 569.
27. G.D. Preston, Nature, Vol. 142, (1939) 570.
28. J.M. Silcock, T.J. Heal and H.K. Hardy, J. Inst. Met., Vol. 82, (1953-54) 239.
29. H. Yoshida, D.J.H. Cockayne and M.J. Whelan, Philos. Mag., Vol. 34, (1976) 89.
30. H.K. Hardy, J. Inst. Met., Vol. 79, (1951) 321.
31. H.K. Hardy, ibid., Vol. 82, (1953-54) 236.
32. J.M. Silcock, T.J. Seal and H.K. Hardy, ibid., Vol. 84, (1955-56) 23.
33. J.D. Boyd and R.B. Nicholson, Acta Metall., Vol. 19, (1971) 1101.
34. R. Sankaran and C. Laird, Mater. Sci. Eng., Vol. 14, (1974) 271.
35. M. Kanno, H. Suzuki and O. Kanoh, J. Japan Inst. Met., Vol. 44, (1980) 1139.
36. J.B.M. Nuyten, Acta Met., Vol. 15, (1967) 1765.
37. B. Parsons and J.M. Silcock, 'Precipitation in Metals', Fulmer Research Institute Special Report No. 3, (1963) 19.
38. A. Garg, Y.C. Chang and J.M. Howe, Scripta Metall. Mater., Vol. 24, (1990) 677.
39. R.W. Fonda, W.A. Cassada and G.J. Shiflet, Acta Metall. Mater., Vol. 40, (1992) 2539.
40. R.J. Chester, Ph.D Thesis, Monash University, Clayton, Vic., Australia (1983).
41. J.M. Silcock, J. Inst. Met., Vol. 89, (1960-61) 203.
42. S.P. Ringer, B.C. Muddle and I.J. Polmear, Proc. 3rd Int. Conf. on Aluminium Alloys (ICAA-3), (L. Arnberg, O. Lohne, E. Nes and N. Ryum, eds.), NTH-SINTEF, Trondheim, Norway, Vol. I, (1992) 214-19, .
43. H.K. Hardy and J.M. Silcock, J. Inst. Met. Vol. 84, (1955-56) 423.
44. G.B. Brook, 'Precipitation in Metals', Fulmer Research Institute Special Report No. 3, (1963)
45. T.H. Sanders Jr. and E.A. Starke Jr., Acta Metall., Vol. 30, (1982) 927.
46. W.A. Cassada, G.J. Shiflet and E.A. Starke Jr, Metall. Trans. A, Vol. 22A, (1991) 299-306.
47. J.M. Howe, J. Lee and A.K. Vasudevan, Metall. Trans. A, Vol. 19A, (1988) 2911-26.
48. S.P. Ringer, K.S. Chee, B.C. Muddle and I.J. Polmear, Proc. 3rd Int. Conf. on Aluminium Alloys (ICAA-3), (L. Arnberg, O. Lohne, E. Nes and N. Ryum, eds.), NTH-SINTEF, Trondheim, Norway, Vol. II, (1992) 9-14.
49. K. Hono, N. Sano, S.S. Babu, R. Okano and T. Sakurai, Acta Metall. Mater., Vol. 41, (1993) 829.
50. G.B. Brook and H.B. Hatt, The Mechanism of Phase Transformations in Crystalline Solids, Inst. of Metals, London, (1969) 82.
51. G.B. Brook, Aircraft Engineering, No. 1, (1975) 32.
52. S. Swenser, S. P. Ringer, B.C. Muddle and I.J. Polmear, Unpublished Research, Monash

University, (1993).
53. L.F. Mondolfo, Metall. Reviews, Rev. No. 153, Joint Publn. Inst. of Metals, Iron and Steel Inst. and Inst. of Metallurgists, (1971) 95-124.
54. W.L. Fink and L. A. Willey, Trans Amer. Inst. of Min. Met. Eng., Vol. 124, (1937) 78.
55. I.J. Polmear, J. Inst. Met., Vol. 86, (1957-58) 113.
56. I.J. Polmear, ibid., Vol. 87, (1958-59) 24.
57. I. J. Polmear, ibid., Vol. 89, (1960-61) 193.
58. J. T. Vietz, K.R. Sargant and I. J. Polmear, ibid., Vol. 92, (1963-64) 327.
59. J.D. Embury and R.B. Nicholson, Acta Metall., Vol. 13, (1965) 403.
60. R. Graf, J. Inst. Met., Vol. 86, (1957-58) 534 (Discussion).
61. G. Thomas, ibid., Vol. 86, (1957-58) 536 (Discussion).
62. G. Thomas and J. Nutting, ibid., Vol. 88, (1959-60) 81.
63. C.W. Morely and B.D. Burns, Nature, Vol. 185, (1960) 914.
64. J. Gjønnes and C.J. Simensen, Acta Metall., Vol. 18, (1970) 881.
65. L.F. Mondolfo, N.A. Gjostein and B.W. Levinson, J. Metals, Trans AIME, Vol. 13, (1956) 1378.
66. J.H. Auld and S. McK. Cousland, J. Aust. Inst. Metals, Vol. 19, (1974) 194.
67. J. Hèrenguel, Rev. Mèt., Vol. 44, (1947) 77.
68. R.C. Chadwick, N.B. Muir and H.B. Grainger, J. Inst. Met., Vol. 85, (1956-57), 161.
69. S. Kerry and V.D. Scott, Metals Sci., Vol. 18, (1984) 289.
70. S.P. Ringer, B.C. Muddle and I.J. Polmear, Acta Metall. Mater., in press, (1993).
71. A. Garg and J.M. Howe, Acta Metall. Mater., Vol. 39, (1991) 1925.
72. K. Hono, T. Sakurai and I.J. Polmear, Scripta Metall, in press, (1993).
73. Y.S. Lee, Unpublished Research, Monash University, (1992-93).
74. S.P. Ringer, B.C. Muddle and I.J. Polmear, Metall. Trans., to be submitted (1994).
75. K.S. Kumar, S.A. Brown and J.R. Pickens, Scripta Metall, Vol. 24, (1990) 1245.
76. S.R. Arumalla and I.J. Polmear, Proc. 7th Intl. Conf. on Strength of Metals and Alloys, (H.J. and M.G. Akben, eds.), Pergamon Press, McQueen, J-P. Bailon, J.I. Dickson, J.J. Jonas Toronto, Vol. 1, (1985) 453.
77. H.R. Shercliff and M.F. Ashby, Acta Metall. Mater., Vol. 38, (1990) 1789-1802.
78. E. Hornbogen and E.A. Starke Jr., Acta Metall. Mater., Vol. 41, (1993) 1-16.
79. J.M. Howe, U. Dahmen and R. Gronsky, Philos. Mag., (1987) 31-61.
80. Aerospace Structural Materials Handbook, U.S. Department of Defense, (1984).
81. R. Devaley, Metals and Materials, Vol. 6, (1972) 404.

Dr. B.C. Muddle

B.Sc. (Hons I) 1971, Ph.D. (Metallurgy), University of N.S.W., 1975

Dr. Muddle has held Postdoctoral Research Fellowships at the University of N.S.W. (1975-6) and the University of Cambridge (1976-8), and was Assistant Professor in the Departments of Metallurgy and Mining Engineering, and Mechanical and Industrial Engineering at the University of Illinois (1979-1983). He joined the Department of Materials Engineering, Monash University in 1983 and is currently Reader in Materials Engineering. His research interests include solid state phase transformations, structure-property relationships in high strength aluminium alloys and continuously cooled steels, microstructure of advanced ceramics, rapid solidification processing of crystalline and amorphous alloys, and applications of analytical electron microscopy.

Dr. S.P. Ringer

B.App.Sc. (Metallurgy), S.A.I.T., 1986
Ph.D. (Materials Science and Engineering), University of N.S.W., 1991

Dr. Ringer was Research Fellow in the Department of Materials Engineering, 1991-93, and is currently Japan Society for the Promotion of Science (JSPS) Research Fellow, Institute for Materials Research, Tohoku University, Sendai, Japan. His research interests include solid state phase transformations, the effect of trace elements on precipitation behaviour in aluminium alloys, and structure-property relationships in high strength aluminium alloys and high strength, low alloy steels.

Professor I.J. Polmear

B. Met.E., M.Sc., D.Eng. (Metallurgy), (University of Melbourne), 1965

Founding Chairman of the Department of Materials Engineering, Monash University and formerly Deputy Vice-Chancellor (Research), Monash University, Professor Polmear is currently Professor Emeritus in the Department of Materials Engineering. He is the author of the highly regarded monograph 'Light Alloys: Metallurgy of the Light Metals' and his long term research interests have focused on the physical metallurgy of the alloys of aluminium, magnesium and titanium, and their applications.